Exploration and Synthesis of Fluorescent Oxadiazole and Thiadiazole Boronyls

A Thesis
SUBMITTED TO THE FACULTY OF THE
UNIVERSITY OF MINNESOTA – DULUTH
BY

Samuel F. Stadem

IN PARTIAL FULFILLMENT OF THE REQUIREMENTS
FOR THE DEGREE OF
MASTER OF SCIENCE

Prof. Paul Kiprof, Advisor

September 2020

Acknowledgements

I would like to thank my advisor, Dr. Paul Kiprof, for his support and assistance over the past three years. He has always had an open door for questions and spared time to help—even when I went on tangents. I would also like to thank Dr. Venkatram Mereddy and his group for a great deal of insight and guidance on many organic synthesis techniques. While I wish I could say all their help led to useful results, I always walked away learning something new. I would also like to thank Marcy Merritt, without whom the lab would be in much worse shape. Finally, I'd like to thank my parents, without whom I'd never have been able to come this far.

Abstract

In the last decade, OLEDs have become increasingly ubiquitous in the market, already available in top-range monitors, televisions, and mobile phones. With the push for cheaper devices, much research has focused on finding new dopants to be used in these displays. Simple azole-based organoboron dyes have shown promise in this application, and our lab has investigated tetra-coordinated boron complexes of the oxadiazole and thiadiazole family. These ligands were chosen for their excellent electron transport capability and ability to make use of boron's unique capability to form B(N,O)X type complexes. Our investigation focused on limiting the rotational sources of internal quenching, and some evidence suggests a notable bathochromic shift when chelated to with BPh_2 while chelation to BF_2 showed signs of a hypsochromic shift. Unfortunately, a lack of suitable instrumentation forced an end to the exploration of thiadiazole complexes. The onset of COVID-19 further stymied compound characterization, though NMR and limited fluorescence spectroscopic data on BPh_2(ODP) was collected.

Table of Contents

List of Figures

List of Tables

List of Schemes

Abbreviations

2,2-HODN	**2,2'-(1,3,4-oxadiazole-2,5-diyl)bis(naphthalen-1-ol)**
3,3-HODN	**3,3'-(1,3,4-oxadiazole-2,5-diyl)bis(naphthalen-2-ol)**
Alq_3	**8-hydroxyquinoline aluminum**
BODIPY	**Boron dipyrromethene**
CRT	**Cathode Ray Tube**
DCM	**Dichloromethane**
DMF	**Dimethylformamide**
DMSO	**Dimethyl sulfoxide**
EDG	**Electron Donating Group**
EIL	**Electron Injection Layer**
EML	**Emissive Layer**
ETL	**Electron Transport Layer**
EWG	**Electron Withdrawing Group**
GCMS	**Gas Chromatography Mass Spectroscopy**
HIL	**Hole Injection Layer**
HTL	**Hole Transport Layer**
HOMO	**Highest Occupied Molecular Orbit**
HODP	**2,2'-(1,3,4-oxadiazole-2,5-diyl)diphenol**
HPOP	**2-(5-phenyl-1,3,4-oxadiazol-2-yl)phenol**
HPTP	**2-(5-phenyl-1,3,4-thiadiazol-2-yl)phenol**
HTDP	**2,2'-(1,3,4-thiadiazole-2,5-diyl)diphenol**
HTL	**Hole Transport Layer**
ITO	**Indium tin oxide**
IPS	**In-Plane Switching**
LCD	**Liquid Crystal Display**
LCMS	**Liquid Chromatography Mass Spectroscopy**
LED	**Light Emitting Diode**
LUMO	**Lowest Unoccupied Molecular Orbit**
MOM	**Methoxymethyl**

NMR	**Nuclear Magnetic Resonance**
OLED	**Organic Light Emitting Diode**
PLED	**Polymer Light Emitting Diode**
TFT	**Thin-film transistor**
THF	**Tetrahydrofuran**
UMD	**University of Minnesota-Duluth**
UV	**Ultraviolet**

Chapter 1

1.1: Boron History and Overview

Boron has a long use in human history, mostly in the form of borax. Also known as sodium borohydrate, the earliest reliable accounts of the use of this compound date back to 762 CE, coming out of the seasonal lake beds in Tibet.[1] It was brought by Arabian traders via the Silk Road as "tincal" to locations such as Mecca, Bagdada, and Medina, where it was used as flux by gold and silversmiths.[2,3] Some evidence suggests its use as far back to ancient Babylonian and Egypt, where it was used in their mummification process; however, such ancient use is not well supported.[2,3] Until its isolation, boron was limited to a handful of niche borax uses such as metal flux and in ceramic glazes.[2,4] The 19th century saw boron being isolated with increasing purity, starting in 1808, and increasing to 98% purity in 1892 by Henri Moissan.[5] Such high purity allowed for greater exploitation of boron's unique properties.

Boron is naturally found in two isotopes, ^{10}B and ^{11}B, roughly in a 1:4 ratio, though the natural abundances varies based on geography.[6] Like the other Group 13 elements, boron is electron deficient, having only three valence electrons in $2s^2 2p^1$ while in the ground state.[3] Boron thus tends towards covalent bonds, and features a tremendous variety of compounds that is only rivaled by carbon.

Of the two natural isotopes, boron-10 is the least abundant and features a large neutron cross section for low-energy neutrons (**Figure 1**). The neutron capture of ^{10}B leads to the formation of ^{4}He and ^{7}Li as its daughter products and usually includes gamma radiation (**Scheme 1**).

As stable daughter elements, there is no further decay heat from the reaction. While several other elemental isotopes have much greater neutron cross sections for thermal neutron—such as ^{113}Cd, ^{149}Sm, ^{151}Eu, and ^{157}Gd—they are all rare-earth elements and found in smaller quantities than boron.[8]

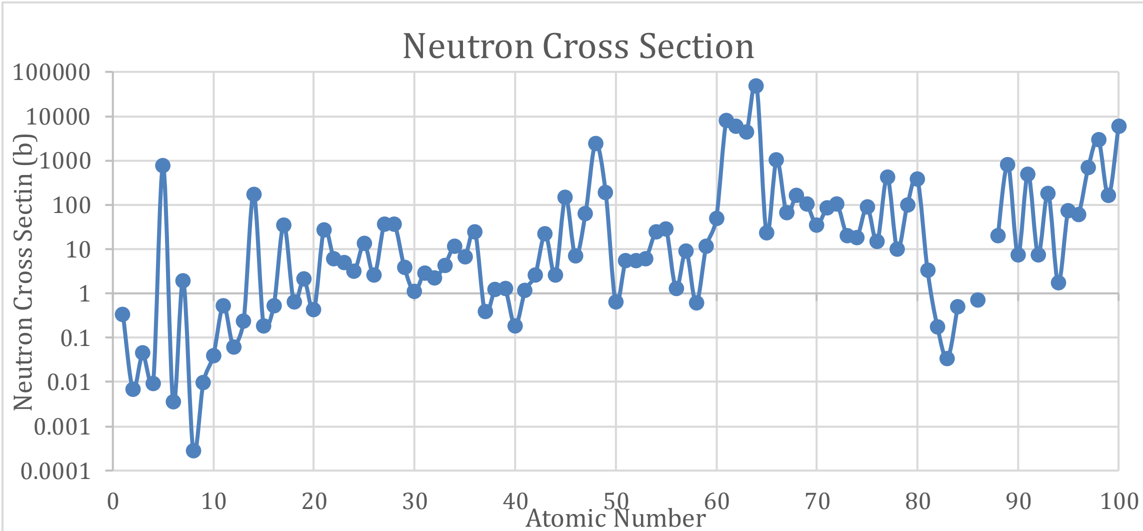

Figure 1 Elemental neutron cross section

The combination of abundance and neutron cross section sees boron used heavily by the nuclear industry in control rods. Boron-10's high neutron cross section has also found use in radiation therapy. This was first proposed in 1936 by G. L. Locher[9], though there were no clinical trials until the 1950s.[10] Thermal neutrons are too low energy to cause damage to tissue, limiting the radiated area to the short range of the resulting α particle penetration. The largest hurdles in this technique have come from selective uptake of the boron into cancerous cells

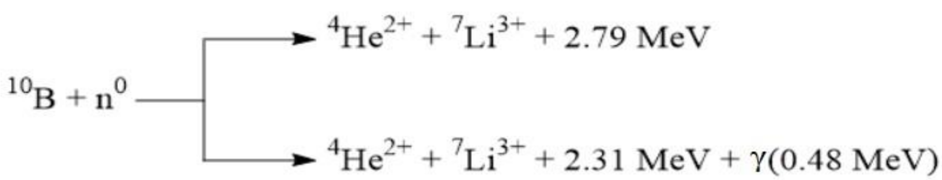

Scheme 1 Boron-10 neutron capture

and attaining sufficient concentration within those cells.[11] The original trials in the 1950s used borax as the delivery agent, but this failed to provide necessary tissue specificity, and trials were halted in 1961 as there was little improvement in patient survival rates. More promising delivery agents are currently under evaluation, such as boron nitride nanotubes, which has been gaining attention since their initial evaluation in 2008.[12,13] BNNTs promise to deliver high concentration of boron per cell with the ability to customize selectivity by attaching different peptides or amino acids to the nanostructure surface, promises that most borated compounds struggle to deliver.[14]

1.2: Boron Chemical Properties

Boron's synthetic reagent applications include hydroboration, allylboration, enolboration, and Suzuki reactions (**Scheme 2**). The highly stereospecific and enantiospecific nature of many of these reactions have made them invaluable in organic synthesis.[15-17] These applications are fueled by boron's unique combination of Lewis acid character, electron deficiency, and strong σ covalent bonding.

Like other group 13 elements, boron has three valence electrons in its ground state; during bonding these electrons combine into an sp^2 hybridized trigonal planar geometry, two electrons short of a full quartet. This, combined with its

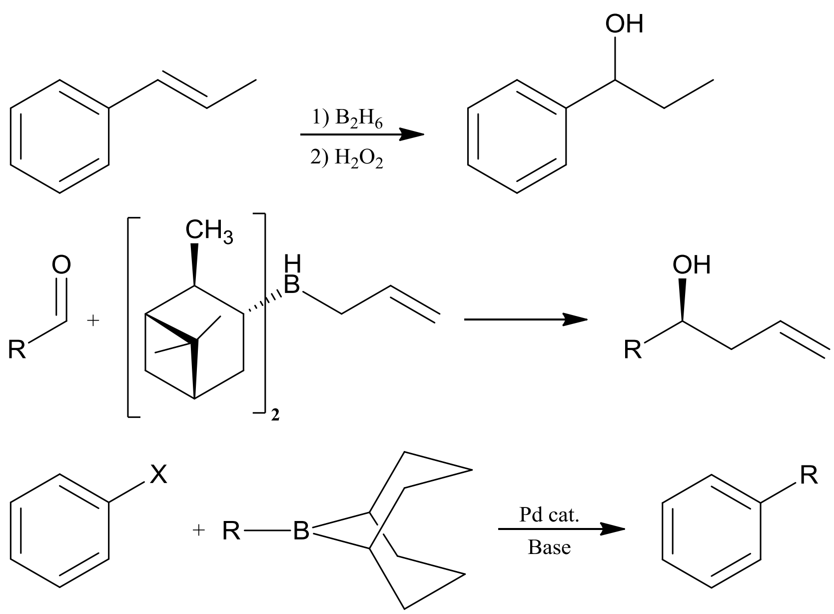

1

2

3

Scheme 2 Examples of hydroboration **(1)**, enolboration **(2)**, and Suzuki coupling **(3)**

small atomic size and high charge density lead to higher ionization energies and greater covalent bonding character than the other elements in its group. [18,19] Boron will also accept electron density to its empty p_z orbital, forming a dative bond and shortening its σ-bonds.[20,21] When boron is thus chelated by a dative bond, it may be locked into tetrahedral geometry. Most of these chelates are N,N or N,O coordinated complexes. This phenomenon is particularly well studied in boron-nitrogen bonds (**Figure 2**), with many properties analogous to alkenes.[22]

In aromatic systems, these aminoborane bonds become isoelectric with alkene systems, though the electronegative differences between boron and nitrogen leaves it open to nucleophilic attack.[23]

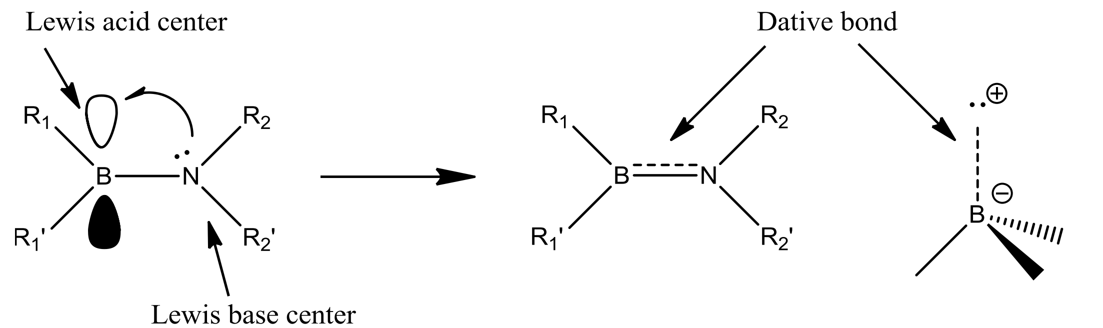

Figure 2 The Lewis acid/base pairing of boron-nitrogen dative bonding **(left)** and tetrahedral boron **(right)**

A rather novel application of this electron density donation has been the exploration of true boron-boron triple bonds. Earlier exploration into group 13 triple bonds found the true bond order to be lower due to severe trans bend in the bonds.[24-25] Boryne dimers are further complicated by the population of the antibonding σ* molecular orbitals, reducing effective bond order.[26] The first example of a diboryne used the strong dative bonding of carbon monoxide acting as a Lewis base to fill the π bonding orbitals, though this compound could only be isolated under laboratory conditions under argon at 8 K (**Figure 3**).[27] More recently, N-heterocyclic carbene (NHC) was used to produce a boryne dimer that is thermally stable at temperatures up to 234°C, opening up the doors to the chemistry of borynes.[28]

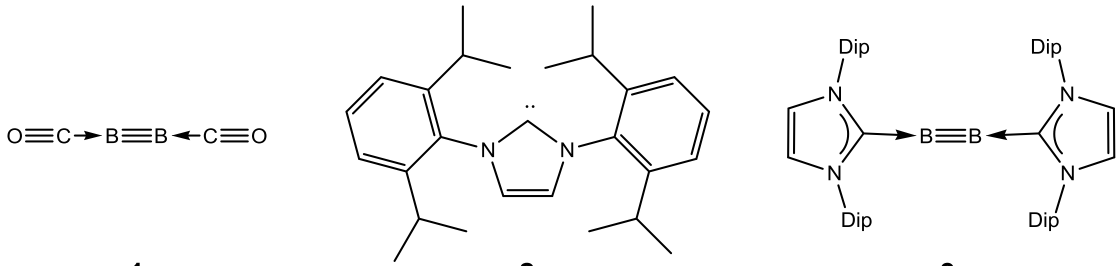

1 2 3

Figure 3 The first diboryne (**1**), the NHC ligand (**2**), and the resulting thermally stable diboryne (**3**)

1.3: Oxadiazoles and Thiadiazoles

Oxadiazoles and thiadiazoles are members of the heterodiazole family of five-member heterocyclic compounds, containing two sp^2 hybridized nitrogen atoms alongside an oxygen or sulfur atom, respectively. Both groups have four isomers, three of which are stable (**Figure 4**).

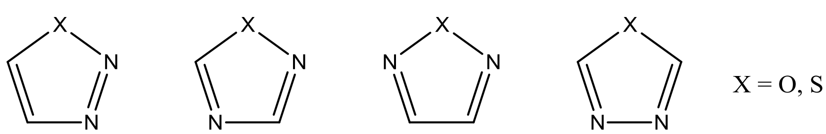

1 2 3 4

Figure 4 The 1,2,3 diazole isomer (**1**), 1,2,4 diazole isomer (**2**), 1,2,5 diazole isomer (**3**), and the 1,3,4 diazole isomer (**4**)

The 1,2,3-oxadiazole isomer is unstable, isomerizing to α-diazoketone (**Scheme 3**).[29] While 1,2,3-oxadiazoles are not isolatable thanks to the ring's instability, its thiadiazole counterpart is in stable equilibrium with its diazothiaketone.[46] These classes of compounds have found a multitude of applications, with oxadiazoles being used in antifungal[30], antiinflamatory[31-33], antitumor[34], antioxidant[35], psychostimulant[36], thermal printing dyes[37], and fluorescent whitening[38] agents. Thiadiazoles have seen use in antibacterial[39-41], antiviral[42], antifungal[43,47], antiplatelet[44], antihypertension[45], and lubricants[43].

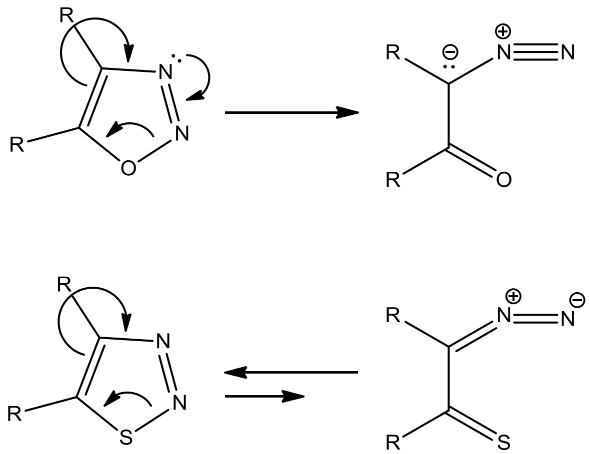

1

2

Scheme 3 The isomerization of 1,2,3-oxadiazole into α-diazoketone (**1**) and the equilibrium of 1,2,3-thiadiazole with α-diazothiaketone (**2**)

A large body of work has come to surround these classes of molecules thanks to their wide array of biological potential.[48,49]

The electron deficiency of the ring makes it an excellent scaffold for luminescent compounds; they are easily tuned by attaching EWG or EDG to moiety, or by extending the π system.[50] The π system may be extended by increasing the conjugation of the system—typically with aromatic systems—or by complexing with metal atoms (**Figure 5**).[50-53]

1 2 3 4

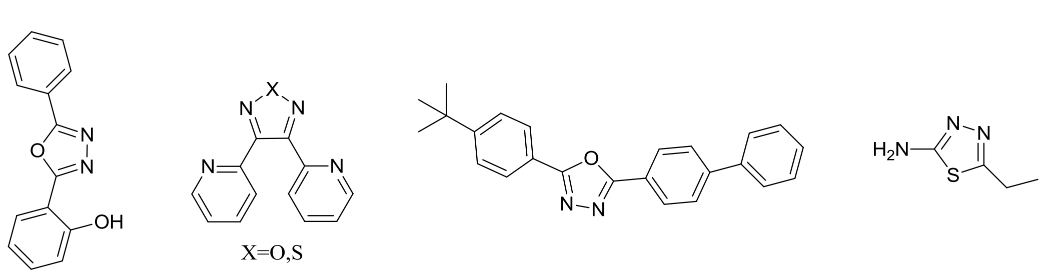

Figure 5 Various luminescent oxadiazole and thiadiazole ligands complexed with aluminium (**1**)[50], palladium and copper (**2**)[51], tin (**3**)[52], and zinc (**4**)[53], respectively

This has seen both oxadiazoles and thiadiazoles used in optics, chemosensors, and OLEDs, including the emerging field of phosphorescent OLEDs.[54]

Chapter 2

2.1: Overview of Liquid Crystal Displays

Since the mid 2000's, LCDs have come to replace CRTs as primary display device for TVs and computer monitors.[55-57] Furthermore, they are the primary display on all mobile devices, dating as far back as the Microvision of 1979. Despite earlier predictions in 1998 that LCDs would soon be replaced due to their limitations, they have managed to dominate the field.[58] However, OLEDs are poised to replace LCDs in the mobile phone and monitor market, and as of 2019 companies such as Samsung and Apple are already offering OLEDs on their top-range phone models.

Current LCDs work by shining a backlight through an initial layer of polarized glass, which then must pass through a layer of liquid crystals. These crystals circularly polarize light to align with a second polarizing layer that is oriented orthogonally to the first (**Figure 6**).[59] TFTs are used to control the circular polarization of the liquid crystals, which physically twist to align themselves with the applied electric field. Color is provided by filters placed between the liquid crystals and the second polarizer.

This construction sets several limitations on the technology. Notable are the energy requirements due to the backlight, response time, viewing angle restrictions, and contrast limitations. Light bleed, caused by a combination scattering from the internal layers and incomplete polarization, means that contrast ratios.[60,61] The polarized light also cause grey levels change with viewing angle.[62] The liquid crystals take time to align themselves to the applied field from the electrodes; being a mechanical process, there is lag between the current being applied and the crystals changing their alignment. This manifests as “ghosting” during fast movement of objects on the screen.[63]

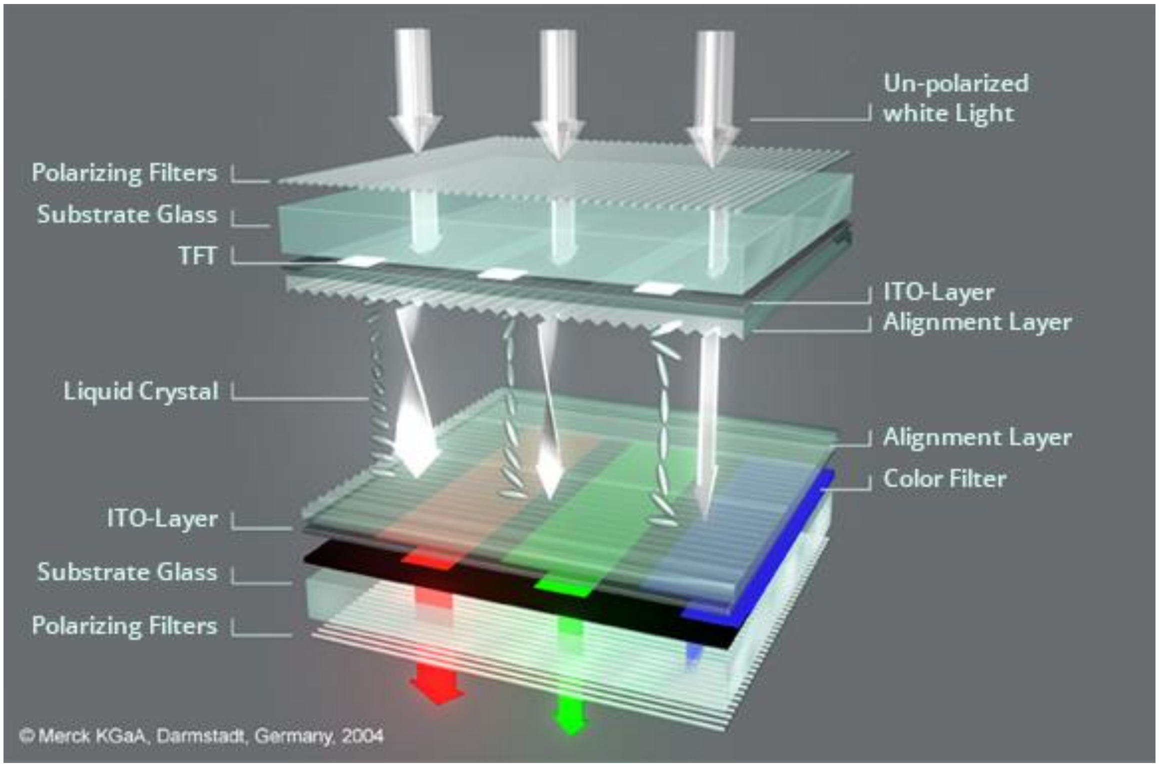

Figure 6 Standard layers of LCDs[64]

Finally, the backlight is always on during operation, even on dark scenes, and represents a constant power drain.

2.2: Overview of Organic Light Emitting Diodes

Organic luminescence devices have been pursued since the 1960's, using a single anthracene layer between two electrodes.[65] Their function is similar to silicon-based LEDs, which have been in use since the early 1970s, which perate on electroluminescence, where a current passing through a semiconductor induces photon emission.

At the cathode, electrons are injected into the LUMO of the diode material and the cathode removes electrons—creating a “hole”—in the HOMO of the diode material (**Figure 7**).[66]

The recombination of hole and electron results in an exciton, or excited atom or molecule, and the return to a ground state releases a photon.

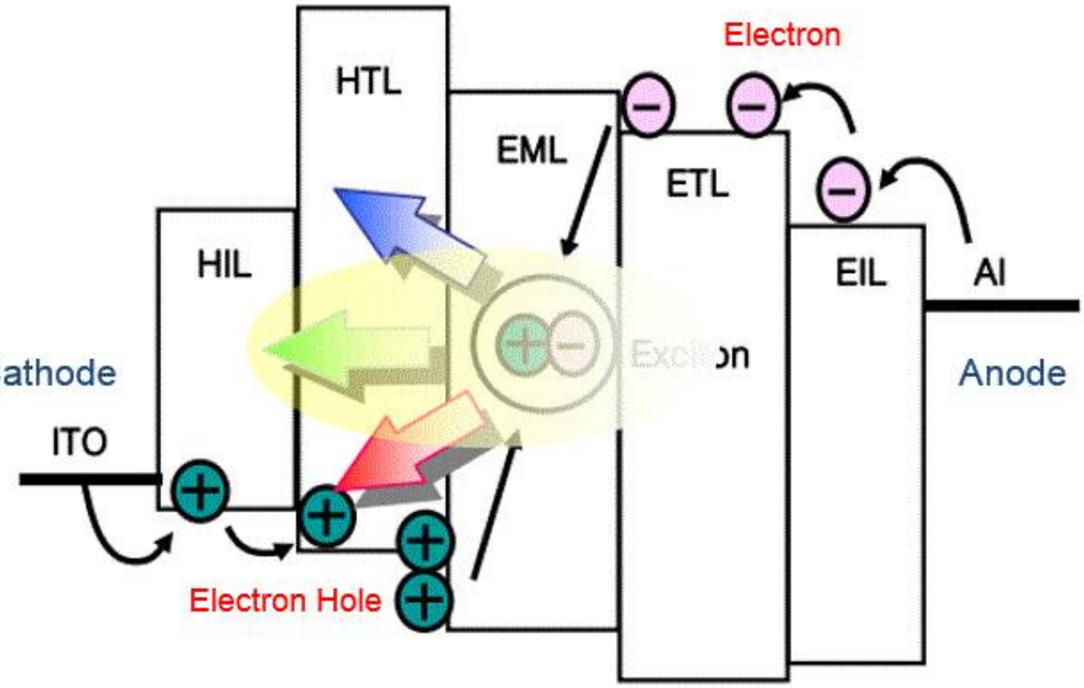

Figure 7 The energy states of OLED layers, and the charge recombination in the EML that produces light[67]

The energy difference between the HOMO and LUMO levels is known as the band gap, and correlates to the wavelength of the emission.[68] In traditional semiconductors, the band gap can be controlled through p-doping and n-doping, where Group 13 and 15 elements are added as impurities to either create electron deficiencies (p-doped) at the cathode or electron surpluses (n-doped) at the anode, respectively.[66]

Organic LEDs operate in a similar manner, using organic materials with good electron mobility in place of n-doped semiconductors and materials with good hole mobility in place of p-doped semiconductors.[69] The first diodes were of a simple single-layer anthracene construction, 5mm thick due to limitations in ultrafilm deposition technology of the time.[65] While proving the concept, the driving voltage ranged from 100 to 1000V and produced poor luminescence.

Later advancements used improved deposition techniques to reduce layer thickness to 50 μm, but with driving voltages remained too high for consumer use.[70,71] The use of 8-hydroxyquinoline aluminum (Alq_3) as an emissive layer by Tang and VanSlyke finally provided a diode functioning at useful voltages, as low as 2.5V.[72] To prevent recombination of charge at the cathode—a problem the first diodes faced—diamine was added as a hole transport, and the layers were kept 135 nm thick.

While the two-layer system has continued to remain prevalent in PLEDs, small molecule OLEDs add an ETL next to the anode, sandwiching the EML (**Figure 8**).[73]

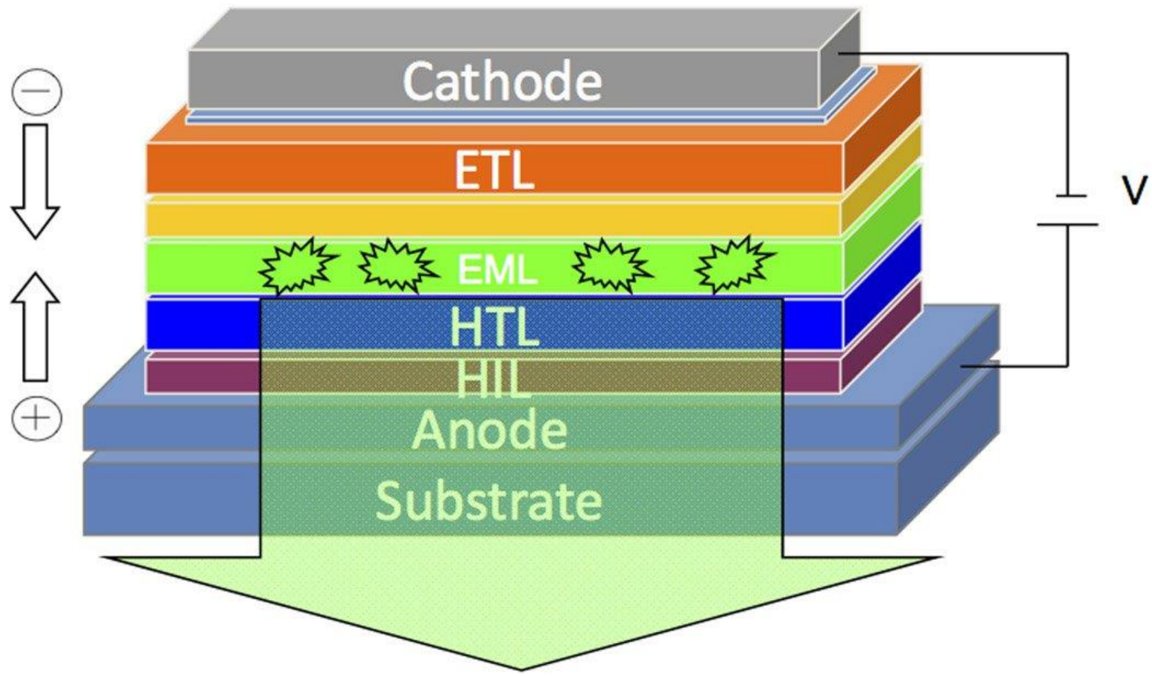

Figure 8 Structure of a simple OLED[74]

Many OLEDs also feature two additional layers to the diode: the Hole Injection Layer (HIL)—situated between the HTL and cathode, and the Electron Injection Layer (EIL), situated between the anode and the ETL.

2.3: Comparison of LCDs and OLEDs

As transmissive devices, OLEDs provide several advantages over LCDs. The most obvious is the lack of a power-draining backlight, along with the restrictive view angles that polarizing filters produce. A less obvious advantage is the improved contrast ratios; while LCD technology such In-Plane Switching and Super Patterned Vertical Alignment are able to provide ratios as high as 1000:1 or 10,000:1, OLED black levels have no transmission, effectively making their contrast ratios infinite.[59] This is also related to the layer thickness of OLEDs, which can be as thin as 10 nm per layer, leading to less light scattering and brighter colors, and does not require a glass substrate; transparent polymer substrates are a viable alternative, allowing for a flexible screen.

Despite their advantages, OLEDs remain the minority in the display market, in large part due to their production costs. Like most consumer electronics, these prices are expected to go down, partially thanks to the ability of OLEDs to be inkjet printed.[75] A larger hurdle relates to the dyes themselves: blue is particularly difficult to produce, and the large band gap required in the material decreases its lifetime due to side reactions.[76,77]

2.4: Organoboron Compounds for OLEDs

Boron's unique properties, discussed earlier, makes it ideal for OLEDs. Its empty p_z orbital allows it to extend *π* systems through N,N and N,O chelates enhance photoluminescent qualities of a system.[78,79] The tetrahedral geometry of boron complexes can also lock disparate *π* systems into the same plane. Further, its strong covalent bonding makes it more stable in complexes than aluminium or zinc[80-72], which has led to several boron-substituted derivatives of aluminium luminescent organometallic complexes.[83-86]

Some of the first compounds to explore these qualities in detail have been the BODIPY dyes, a family of N,N chelates[87], as well as related N,O chelates (**Figure 9**).[88,89] However, the BODIPY core has seen limited research into OLED fluorophores.[88,89]

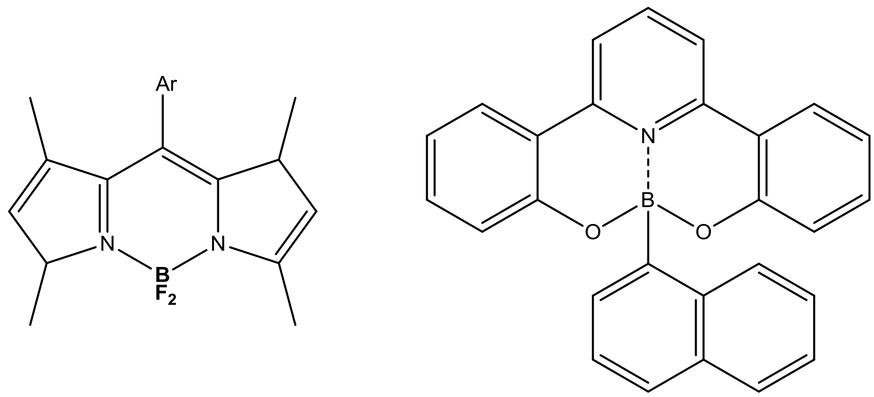

1 2

Figure 9 BOPIDY (**1**) and the related polydentate polypyridine chelate (**2**)

Instead, much focus has been on N,O chelates, often based on Tang and Van Slyke's original Alq_3 scaffold. These BAr_q compounds have proven to be exceptionally tunable by extending the π system, or by attaching either EDG or EWG to the core scaffold.[90,91] Extending the π system and attaching EDG to the core scaffold have proven to have analogous effects of shifting the emissions bathochromically, while attaching EWG shifts emissions hypsochromically.[83,92] The ease at which boron can facilitate charge transfer though its empty p_z orbital has seen it used as an EML, ETL, and even dual-function EML-ETL.[84,85,93,94]

Chapter 3

3.1: Synthesis and Development of HODP and HTDP

Our group has become interested in N,O ligands that build off Tang and Van Slyke's work by replacing the triquinolate with oxadiazoles and thiadiazoles. Early work has shown this to be a promising direction, particularly with the HPOP scaffold.[49] There is little research into the related HPTP scaffold, though previous work by our group suggests a bathochromic shift should be expected.[95]

Our oxadiazole research is based on earlier work by Justin Hines with 1,2-HPON, 2,3-HPON, and HPOP (**Figure 10**).[96]

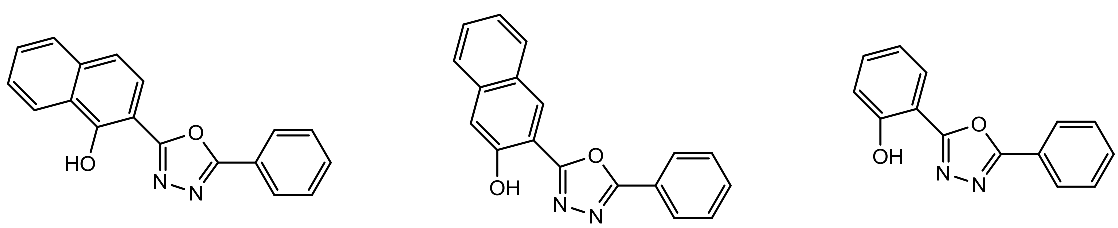

1 **2** **3**

Figure 10 The structures of 1,2-HPON (**1**), 2,3-HPON (**2**), and HPOP (**3**)

Expanding upon that work, locking the free rotation of the phenyl was decided as a logical next step, achieved either through hydrogen bonding or through twin boronyls (**Figure 11**).

Based on similar work by Frath *et al.*, we expected to see stronger Stokes shifts and better quantum yield.[97] This can be attributed to the pseudo-extension of the π complex through boron, and the removal of vibration and rotation as sources of internal quenching.[98,99]

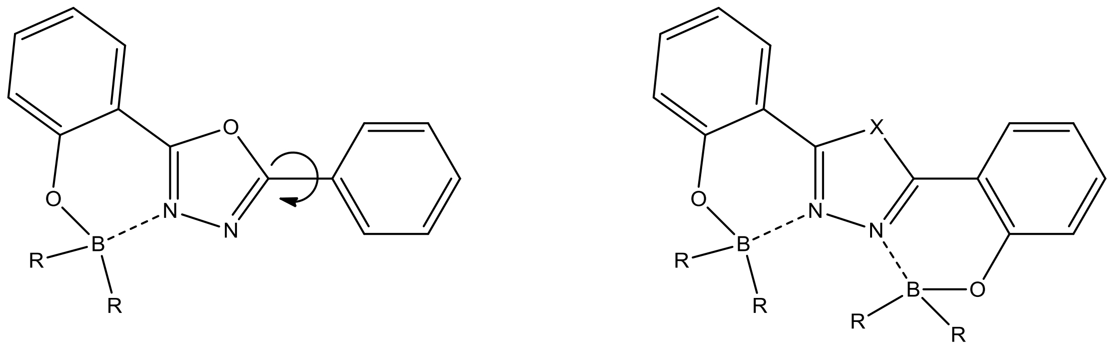

1 2

Figure 11 Rotational source of quenching in the HPOP complex (**1**), locked rotation of the diboronyl complex (**2**)

The first ligand started was HODP, which followed the synthesis of HPOP; this proceeded without incident (**Scheme 4**).

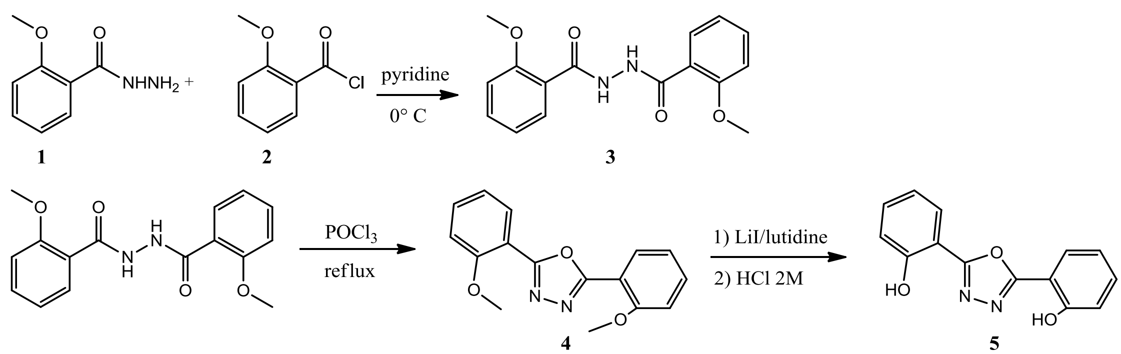

Scheme 4 Synthesis of HODP

Once 2-methoxybenzohydrazide (**1**) was synthesized, 2-methoxybenzoyl chloride (**2**) was substituted for benzoyl chloride, where filtration and washing with 600 mL of water proved to provide more consistent yields of 2-methoxy-N'-(2-methoxybenzoyl)benzohydrazide (**3**) than recrystallization in 75% ethanol. Yields of 2,5-bis(2-methoxyphenyl)-1,3,4-oxadiazole (**4**) sat consistently at 50%, fluorescing blue under 375nm UV light in its solid state. The final HODP ligand (**5**) required four equivalents of lithium iodide and refluxed for at least 24 hours under a dry atmosphere to ensure full hydrolysis; GCMS showed most products were only partially hydrolyzed. Liquid-liquid extraction with DCM was originally used for purification, but the yields were below 50%. Chromatography with silica gel, first with hexane followed by 20% ethyl acetate/toluene, provided better yields. The resulting product was a white powder that fluoresced green under 375 nm UV light, and fluorescent emission in DCM at 446 nm.

3.2 Synthesis of Diphenylboronyl and Difluoroboronyl Complexes

Two boron complexes were planned; diphenylboronyl and difluoroboronyl. Little steric hindrance was expected with difluoroboronyl, allowing a diboron complex that extends the *π* system across the whole molecule. With diphenyl boronyl, the hindrance of the twin phenyl groups was likely to prevent more than one boron to complex with the ligand.

The difluoroboronyl complex was initially synthesized in dry toluene, but no product was produced (**Scheme 5**).

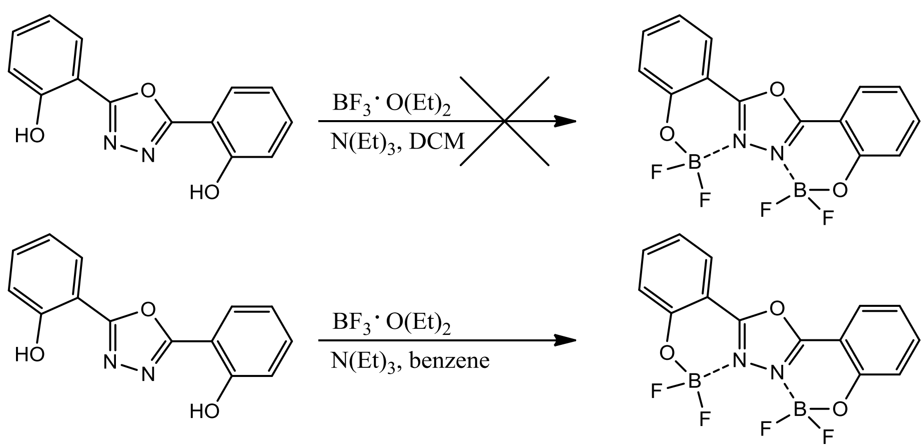

Scheme 5 Synthesis of BF_2(ODP)

Dichloromethane was also used as solvent, but the reaction did not go to completion. Isolating products was also problematic; aqueous conditions could not be used in the extraction due to the hydrolyzing of the boronyl bond. Benzene was found to be the best solvent; excess could be evaporated in vacuo easily and recrystallized in cold benzene. Washing with cold diethyl ether left a white powder that fluoresced a deep blue. The resulting compound showed poor solubility in both THF and acetonitrile, and neither the monoboron nor diboron complex could be identified by LCMS. While these results did not give evidence of the difluoroboronyl complex, the change in fluorescence—a different color than 2,5-bis(2-methoxyphenyl)-1,3,4-oxadiazole—suggested a new unique compound. The poor solubility extended to chloroform, DCM, ethanol, methanol, and DMF, making further spectroscopy difficult.

The synthesis of the diphenylboronyl complex originally made use of dry toluene and diphenylborinic acid produced *in situ* from 2-aminoethyldiphenylborinic acid, then refluxed for two hours (**Scheme 6**). No product was detected, and the compound displayed the same characteristic fluorescent color as HODP, suggesting hydrolysis had reverted the product.

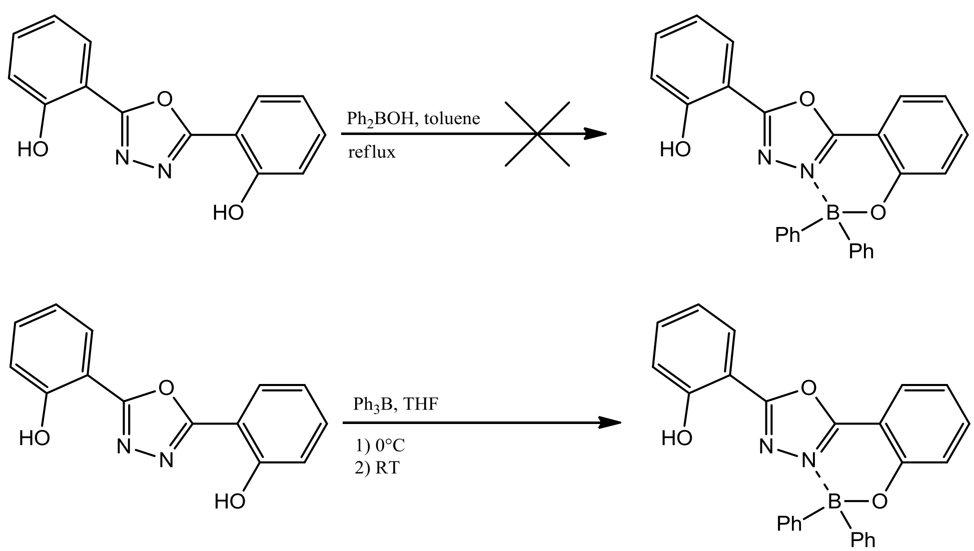

Scheme 6 Synthesis if BPh_2(ODP)

In a second attempt, dry THF was brought to 0°C and triphenyl borane in THF was used as reagent. After letting the reaction come to room temperature over three hour, the resulting complex was easily identifiable by both cursory UV illumination and subsequent spectroscopy. Initial ^{1}H NMR suggested several aromatic and aliphatic impurities were still in the product, though after experimenting with several purification techniques it was found that that washing with hexane and filtering with hot toluene removed most of these impurities. The final product was a yellow powder that fluoresced teal under UV, and was confirmed by LCMS and NMR. Fluorescent emission in DCM was 448 nm and a 35 nm Stokes shift, a minimal 2 nm bathochromic shift. This contrasts to the visible color differences between the diphenyl boronyl complex and the ligand (**Figure 12**).

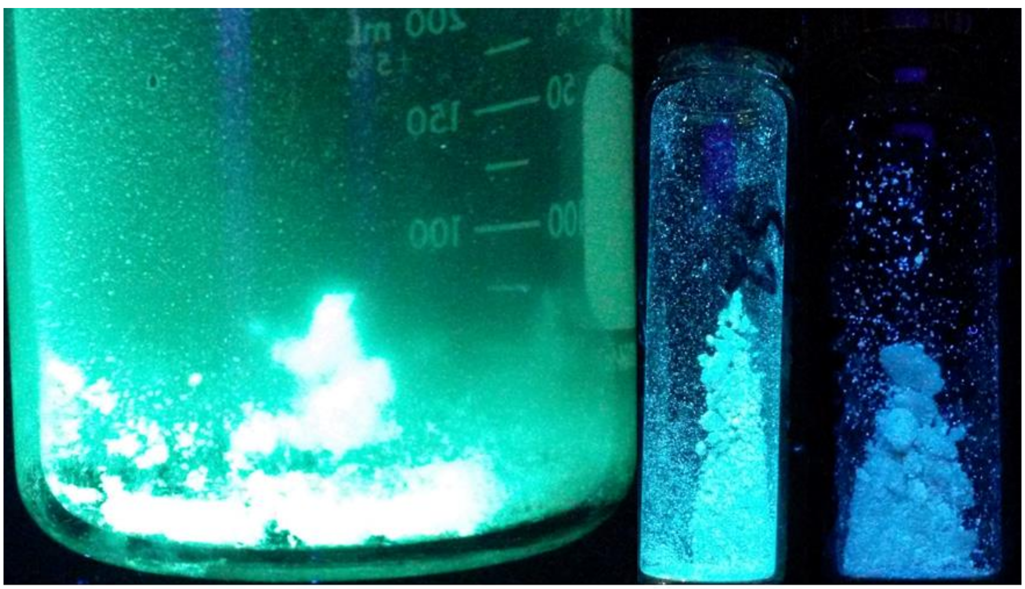

1 2 3

Figure 12 Under UV light, the HODP ligand (**1**), Ph_2(ODP) complex (**2**), and possibly the BF_2(ODP) complex (**3**)

Attempts were also made to synthesize HTDP via microwave synthesis using a legacy CEM Discovery, according to the technique published by Lebrini *et al* (**Scheme 7**).[99] Previous work in our lab showed the oxadiazole boronyl complexes to be susceptible to hydrolysis due to the electron deficiency of the ring. One hope was that the lower electronegativity of sulfur might make the compounds more resilient to hydrolisis. Unfortunately, most reactions produced only trace amounts of the desired product according to GCMS.

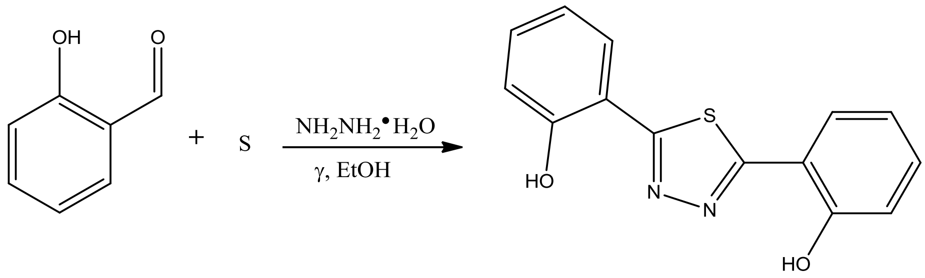

Scheme 7 Synthesis of HTDP

The major product was consistently an iminomethylphenol dimer. Only after changing to a Discovery SP, which allowed the real-time monitoring of reaction pressure, was it realized that the technique required reaction pressure was 30 bars rather than 30 psi. Reaction time was extended in the hopes it might substitute for lower pressure, though reaction results did not change. Further investigation into this potentially useful pathway was abandoned as we did not have a reaction vessel capable of safely handling such pressures.

3.3: Exploration of Naphthalene Extended Oxadiazole Ligands

One last synthesis pathway explored was by extending the *π* conjugate system by substituting naphthalene for the phenyl moiety. Synthesis based on 1-hydroxy-2-naphthoic acid was the primary focus, as this 1,2-HOPN proved to be a better fluorophore in previous work by our group.[96] The short shelf life of lithium iodide, required to hydrolyze the methoxy protection group, prompted some attempts to find alternative ways to protect the hydroxyl group (**Scheme 7**). The resulting product was split between MOM disubstitution and monosubstitution according to GCMS. ^{1}H NMR did not show the presence of any carboxylic acid, suggesting the MOM protection group was not preferentially attaching to the hydroxyl group. A standard benzoate protection was next attempted, with the resulting product a viscous oil. This was not deemed worth the extra synthesis time over methoxy protection and thus discarded, falling back on methoxy protection.

To prepare 2,2-HODN and 3,3-HODN, synthesis of the acid chloride precursor was attempted using 3-hydroxy-2-naphthoic acid under the assumption that only the carboxylic acid would be attacked (**Scheme 8**). Given the water sensitivity of acid chlorides, an *in situ* preparation was deemed the best course. After running the reflux reaction under argon, the final product was a black sludge. Several attempts were made to refine the reaction, but the final product remained a thick oil that did not dissolve in pyridine. Synthesis with 2-methoxybenzoyl chloride proved no more fruitful (**Scheme 8**).

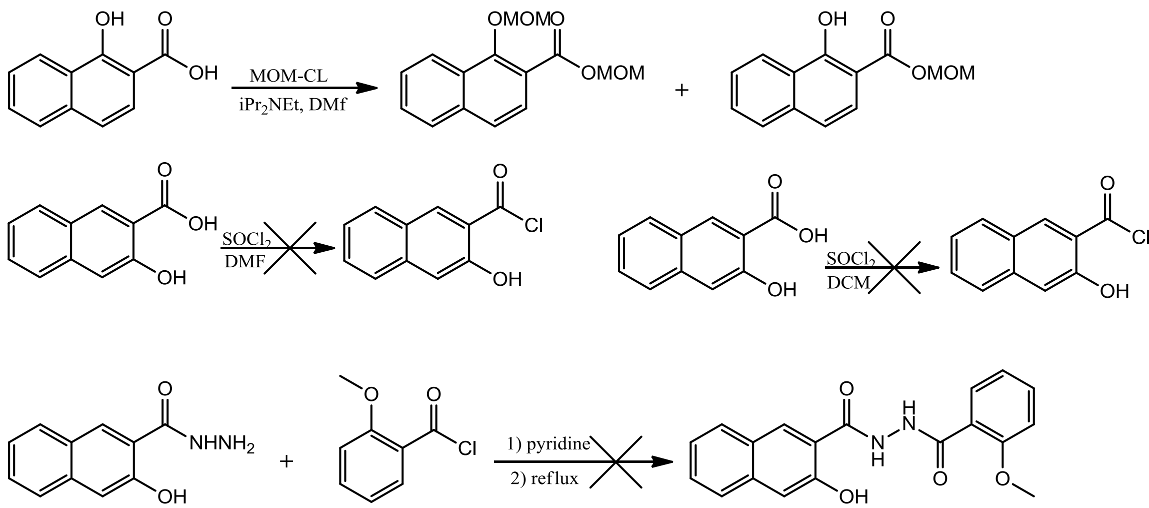

Scheme 8 Synthesis attempts of 2,2-HODN and 3,3-HODN precursors

Initial synthesis was performed in an ice bath and allowed to reach room temperature over 24 hours, which did not produce any measurable product. Further attempts to refine the synthesis included adding a short ten-minute reflux and reacting under argon, though none succeeded in producing any product. The last reaction instead produced two compounds whose masses by GCMS were consistent with a 2-methoxyhydrazide dimer as a minor product and 2-methoxy HPOP as a major product.

3.4: Summary and Conclusions

Our oxadiazole research unfortunately only characterized one boron complex, BPh_2(ODP), with evidence suggesting the creation of BF_2(ODP). The complex of only one diphenylboron to HODP was confirmed by LCMS, confirming suspicions that the diphenyl group was too sterically hindered to allow a diboronyl system. Strong hydrogen bonding was evident in ^{1}H NMR, though it demonstrated a marginal bathochromic shift of 5 nm compared to BPh_2(POP) in THF. The observed fluorescence of the solid state—teal—suggests a greater bathochromic shift that could not be properly explored due to the shutdown brought on by COVID-19. The BPh_2(ODP) chelate displayed only a small 3 nm hypsochromic shift compared the ligand when in DCM, which agrees with EWG shift predictions (**Table 1**).[81,90]

Compound Name	Excitation Wavelength (nm)	Emission Wavelength (nm)
HPOP	387	458
BPh2(POP) (THF)	257, 304, 338, 406	443
HODP (DCM)	365, 391	451
HODP (EtOH)	292, 357	439
BPh2(ODP) (DCM)	263, 302, 350, 413	448
BPh2(ODP) (EtOH)	289, 366	436

Table 1 Excitation and emission wavelengths of oxadiazole ligands and complexes

LCMS could not confirm the presence of the BF_2(ODP) complex, partially due to the poor solubility of the product in most solvents tried. The very obvious shift in fluorescence color under UV light from the ligand to the product strongly suggests a complex was formed, and warrants further investigation.

Though our thiadiazole synthesis could not continue due to our microwave reactor’s inability to sustain the necessary pressures, this is an avenue of research that is worth pursuing due to the potential of finding more water-stable complexes.

Chapter 4

NMR Spectroscopy

All spectra were taken on a Bruker Ascent 400 MHz NMR spectrophotometer at 25°C. The deuterated solvents for each spectrum was referenced to the literature value.

GCMS Spectroscopy

All spectra were taken on an Agilent 7890B GC with an Agilent 5977B MSD.

LCMS Spectroscopy

Spectra were taken on a ThermoScientific Ultimate 3000 LC with an attached Bruker microTOF-QIII MS.

Fluorescence Spectroscopy

All fluorescent spectral data was taken on a Varian Cary Eclipse.

Synthesis of 2-methoxy-N'-(2-methoxybenzoyl)benzohydrazide

In a 50 mL round-bottom flask, 2-methoxybenzohydrazide (4.012 g, 24.14 mmol) was dissolved in pyridine (20 mL) and placed in an ice bath. After being allowed to cool and flushed with argon, 2-methoxybenzoyl chloride (4.80 mL, 32.3 mmol) was dropwise added over 40 minutes. After being allowed to come to room temperature over 2 hours, a reflux was run for 10 minutes before being added to 400 mL ice water. The precipitate was filtered and dried, producing a white powder (4.599 g, 63.4% yield)

Synthesis of 2,5-bis(2-methoxyphenyl)-1,3,4-oxadiazole

In a 100 mL round-bottom flask, 2-methoxy-*N'*-(2-methoxybenzoyl)benzohydrazide (3.844 g, 12.80 mmol) was refluxed with phosphoryl chloride (46.9 mL) over 24 hours. The resulting yellow solution was dropwise added to 400 mL ice water, producing a white precipitate. The precipitate was filtered and extracted by 3x50 mL DCM and dried over magnesium sulfate, producing a white powder that fluoresced blue (2.168 g, 60.0% yield). Process was repeated four additional times.

*Synthesis of 2,2'-(1,3,4-oxadiazole-2,5-diyl)diphenol (**HODP**)*

In a 100 mL Schlenk flask, 2,5-bis(2-methoxyphenyl)-1,3,4-oxadiazole (5.866 g, 20.78 mmol) was dissolved in 2,6-lutidine (30 mL) and flushed with argon. Lithium iodide (7.185 g, 53.68 mmol) was slowly added before the flask was flushed again and heated to reflux. The condenser was attached to a column packed with Dryrite. The column was sealed after reflux started and was allowed to react for 24 hours. The resulting yellow solution was transferred with 50 mL DI water into 100 mL 2M HCl solution. This was extracted by 3x30 mL DCM and 1x30 mL DI water and dried over magnesium chloride. The resulting light brown powder was further purified by column chromatography with hexanes, followed by 20% ethyl acetate/toluene. The final product was a white powder that fluoresced green (3.416 g, 64.7% yield). Most common byproduct was a single methoxy ligand. Refer to appendix for experimental data.

Synthesis of 2-(5-(2-((diphenylboryl)oxy)phenyl)-1,3,4-oxadiazol-2-yl)phenol

In a 50 mL round-bottom flask, HODP (0.265 g, 1.04 mmol) was dissolved in dry THF (20 mL) and cooled in an ice bath for 10 minutes. After flushing with argon, triphenyl borane (0.25M, 5.0 mL) was dropwise added over 40 minutes. After addition, the vessel was sealed and allowed to come to room temperature over 4 hours. Excess THF was removed in vacuo and the resulting solid was washed with hexane and filtered by hot toluene. The remaining solid was a pale yellow that fluoresced teal (0.146 g, 33.6% yield). Refer to appendix for experimental data.

Bibliography

[1] Garrett, D. E. Borates: handbook of deposits, processing, properties, and use, 1st ed.; Academic Press: San Diego, 1998.

[2] Materials World. August 2004, p 26.

[3] Woods, W. G. An Introduction to Boron: History, Sources, Uses, and Chemistry. Environ Health Perspect **1994**, 102 (7), 5–11.

[4] Travis, N. J.; Cocks, E. J. The Tincal Trail: A History of Borax, 1st ed.; Harrap: London, 1984.

[5] Greenwood, N. N.; Earnshaw, A. Chemistry of the Elements, 1st ed.; Pergamon Press Ltd.: Elmsford, NY, 1985.

[6] Sah, R. N.; Brown, P. H. Isotope Ratio Determination in Boron Analysis. Biological Trace Element Research **2013**, 66 (1-3), 39–53.

[7] Encyclopedia of inorganic chemistry, 1st ed.; King, R. B., Ed.; Wiley: Chichester, 1994; Vol. 1.

[8] CRC Handbook of Chemistry and Physics, 97th ed.; Haynes, W. M., Lide, D. R., Eds.; Taylor & Francis Group: Boca Raton, FL, 2017.

[9] Locher, G. L. Biological Effects and Therapeutic Possibilities of Neutrons. Am. J. Roentgenol **1936**, 36, 1–13.

[10] Sweet, L. E.; Robertson, W. H.; Foster, C. G.; Locksley, H. B.; Sutherland, D. L.; Mendelsohn, M. L. Neutron Capture Therapy with Boron in the Treatment of Glioblastoma Multiforme. Am J Roentgenol Radium Ther Nucl Med **1954**, 71 (2), 279–293.

[11] Coder, J. A.; Morris, G. M. The Radiation Biology of Boron Neutron Capture. Radiation Research **1999**, 151 (1), 1–18.

[12] Ciofani, G.; Raffa, V.; Menciassi, A.; Cuschieri, A. Folate Functionalized Boron Nitride Nanotubes and Their Selective Uptake by Glioblastoma Multiforme Cells: Implications for Their Use as Boron Carriers in Clinical Boron Neutron Capture Therapy. Nanoscale Res. Lett. **2008**, 4 (2), 113–121.

[13] Nakamura, H.; Koganei, H.; Miyoshi, T.; Sakurai, Y.; Ono, K.; Suzuki, M. Antitumor Effect of Boron Nitride Nanotubes in Combination with Thermal Neutron Irradiation on BNCT. Bioorganic & Medicinal Chemistry Letters **2015**, 25 (2), 172–174.

[14] Barth, R. F.; Coderre, J. A.; Vincente, M. G.; Blue, T. E. Boron Neutron Capture Therapy of Cancer: Current Status and Future Prospects. Clin. Cancer Res. **2005**, 11 (11), 3987–4002.

[15] Brown, H. C.; Zweifel, G. A Stereospecific Cis Hydration Of The Double Bond In Cyclic Derivatives. Journal of the American Chemical Society **1959**, 81 (1), 247–247.

[16] Brown, H. C.; Bigley, D. B. Bis-3-Methyl-2-Butylborane As A Selective Reagent For The Reduction Of Representative Functional Groups. Journal of the American Chemical Society **1961**, 83 (2), 486–486.

[17] Zweifel, G.; Arzoumanian, H. .Alpha.-Halovinylboranes. Their Preparation and Conversion Into.alpha.-Halovinylboranes. Their Preparation and Conversion into Cis-Vinyl Halides, Trans-Olefins, Ketones, and Transvinylboranes. Journal of the American Chemical Society **1967**, 89 (19), 5086–5088.

[18] Cotton, F. A. Advanced inorganic chemistry; Wiley: New York, **1999**.

[19] Muetterties, E. The Chemistry of Boron and Its Compounds; John Wiley and Sons
Inc: New York, **1967**.

[20] Fujimoto, H.; Satoh, S. Orbital Interactions and Chemical Hardness. The Journal of Physical Chemistry **1994**, 98 (5), 1436–1441.

[21] Hirao, H.; Ohwada, T. Generation of Orbitals That Control Molecular Reactivity: Projected Reactive Orbital Approach. The Journal of Physical Chemistry A **2005**, 109 (33), 7642–7647.

[22] Niedenzu, K.; Dawson, J. W. Boron-Nitrogen Compounds; Springer-Verlag: Heidelberg, **1965**.

[23] *Encyclopedia of Inorganic Chemistry*; King, R. B., Ed.; Wiley: Chichester u.a., 1994; Vol. 1.

[24] Power, P. P. π-Bonding and the Lone Pair Effect in Multiple Bonds between Heavier Main Group Elements. Chemical Reviews **1999**, 99 (12), 3463–3504.

[25] Fischer, R. C.; Power, P. P. ChemInform Abstract: π-Bonding and the Lone Pair Effect in Multiple Bonds Involving Heavier Main Group Elements: Developments in the New Millennium. ChemInform **2010**, 41 (51).

[26] Frenking, G.; Holzmann, N. A Boron-Boron Triple Bond. Science **2012**, 336 (6087), 1394–1395.

[27] Zhou, M.; Tsumori, N.; Li, Z.; Fan, K.; Andrews, L.; Xu, Q. OCBBCO: A Neutral Molecule with Some Boron−Boron Triple Bond Character. Journal of the American Chemical Society **2002**, 124 (44), 12936–12937.

[28] Braunschweig, H.; Dewhurst, R. D.; Hammond, K.; Mies, J.; Radacki, K.; Vargas, A. Ambient-Temperature Isolation of a Compound with a Boron-Boron Triple Bond. Science **2012**, 336 (6087), 1420–1422.

[29] Schweig, A.; Baumgartl, H.; Schulz, R. IR and UV Matrix Photochemistry and Solvent Effects: the Isomerization of Diazocyclohexadienones (Ortho Quinone Diazides) — Detection of Molecules with the 1,2,3-Benzoxadjazole Structure. A UV/Vis and IR Absorption and UV Photoelectron Spectroscopic Investigation. Journal of Molecular Structure **1991**, 247, 135–171.

[30] Srivastava, R. M.; Freire, M. V. S.; Chaves, A. S. C.; Beltrão, T. M.; Carpenter, G. B. Synthesis, Spectroscopic Studies and the Mechanism of Formation of 4,5-Dihydro-1,2,4-Oxadiazoles. Journal of Heterocyclic Chemistry **1987**, 24 (1), 101–105.
[31] Satyanarayana, K.; Rao, M. Synthesis and Antiinflammatory, Analgesic, and Antipyretic Testing of 4-[1-Oxo-(3-Substituted Aryl)-2-Propenyl]-3-Phenylsydnones and of 3-[4-[3-(Substituted ary1)-1-Oxo-2-Propenyl] Phenyl] Sydnones. Journal of Pharmaceutical Sciences **1995**, 84 (2), 263–266.
[32] Palazzo, G.; Tavella, M.; Strani, G.; Silvestrini, B. 1,2,4-Oxadiazoles--IV. Synthesis and Pharmacological Properties of a Series of Substituted Aminoalkyl-1,2,4-Oxadiazoles. Journal of Medicinal and Pharmaceutical Chemistry **1961**, 4 (2), 351–367.
[33] Boschelli, D. H.; Connor, D. T. 1,2,4-oxadiazole and 1,2,4-thiadiazole derivatives of fenamates as antiinflammatory agents. U.S. Patent 5114958, May 19, 1992.
[34] Anto, R. J.; Kuttan, G.; Kuttan, R.; Sathyanarayana, K.; Rao, M. N. A. Tumor-Reducing and Antioxidant Activities of Sydnone-Substituted Chalcones. Journal of Clinical Biochemistry and Nutrition **1994**, 17 (2), 73–80.
[35] Narla, R. S.; Rao, M. N. A. Scavenging of Free-Radicals and Inhibition of Lipid Peroxidation by 3-Phenylsydnone. Journal of Pharmacy and Pharmacology **1995**, 47 (8), 623–625.
[36] Ganiev, M. M.; Kharlamov, A. N.; Raevskii, K. S.; Guseinov, D. Y. Effect of Sydnocarb on Learning and Memory. Bulletin of Experimental Biology and Medicine **1987**, 104 (4), 1413–1415.
[37] Ono, M.; Yasui, S.; Noguchi, A.; Takiguchi, R.; Eguchi, H.; Kafuku, K. Thermal Transfer Recording Dye and Thermal Transfer Sheet. PCT Int. WO1992005032, April 02, 1992.
[38] Schinzel, E.; Martini, T.; Spatzier, W.; Probst, H.; Ger. Pat. Offen. 3126464, 1983.
[39] Maejima, T.; Inoue, M.; Mitsuhashi, S. In Vitro Antibacterial Activity of KP-736, a New Cephem Antibiotic. Antimicrobial Agents and Chemotherapy **1991**, 35 (1), 104–110.
[40] Miyake, A.; Yoshimura, Y.; Yamaoka, M.; Nishimura, T.; Hashimoto, N.; Imada, A. Studies on Condensed-Heterocyclic Azolium Cephalosporins. IV. Synthesis and Antibacterial Activity of 7.BETA.-(2-(5-Amino-1,2,4-Thiadizol-3-Yl)-2(Z)-Alkoxyiminoacetamido)-3-(Condensed-Heterocyclic Azolium)Methyl Cephalosporins Including SCE-2787. The Journal of Antibiotics **1992**, 45 (5), 709–720.
[41] Khalaj, A.; Nakhjiri, M.; Negahbani, A. S.; Samadizadeh, M.; Firoozpour, L.; Rajabalian, S.; Samadi, N.; Faramarzi, M. A.; Adibpour, N.; Shafiee, A.;

Foroumadi, A. Discovery of a Novel Nitroimidazolyl–Oxazolidinone Hybrid with Potent Anti Gram-Positive Activity: Synthesis and Antibacterial Evaluation. European Journal of Medicinal Chemistry **2011**, 46 (1), 65–70.
[42] "The DERWENT Standard Drug File of Known Drugs", Derwent, London, 1994.
[43] Kurzer, F. 1,2,4-Thiadiazoles. Advances in Heterocyclic Chemistry Volume 32 Advances in Heterocyclic Chemistry **1982**, 285–398.
[44] Thomas, E. W.; Nishizawa, E. E.; Zimmermann, D. C.; Williams, D. J. Synthesis and Platelet Aggregation Inhibitory Activity of 4,5-Bis(Substituted)-1,2,3-Thiadiazoles. Journal of Medicinal Chemistry **1985**, 28 (4), 442–446.
[45] Chapleo, C. B.; Myers, P. L.; Smith, A. C. B.; Stillings, M. R.; Tulloch, I. F.; Walter, D. S. Substituted 1,3,4-Thiadiazoles with Anticonvulsant Activity. 4. Amidines. Journal of Medicinal Chemistry **1988**, 31 (1), 7–11.
[46] Eicher, T.; Hauptmann, S.; Speicher, A. The Chemistry of Heterocycles Structures, Reactions, Synthesis, and Applications, 3rd ed.; Wiley: Weinheim, 2012.
[47] Chen, C.-J.; Song, B.-A.; Yang, S.; Xu, G.-F.; Bhadury, P. S.; Jin, L.-H.; Hu, D.-Y.; Li, Q.-Z.; Liu, F.; Xue, W.; Lu, P.; Chen, Z. Synthesis and Antifungal Activities of 5-(3,4,5-Trimethoxyphenyl)-2-Sulfonyl-1,3,4-Thiadiazole and 5-(3,4,5-Trimethoxyphenyl)-2-Sulfonyl-1,3,4-Oxadiazole Derivatives. Bioorganic & Medicinal Chemistry **2007**, 15 (12), 3981–3989.
[48] Hu, Y.; Li, C.-Y.; Wang, X.-M.; Yang, Y.-H.; Zhu, H.-L. 1,3,4-Thiadiazole: Synthesis, Reactions, and Applications in Medicinal, Agricultural, and Materials Chemistry. Chemical Reviews **2014**, 114 (10), 5572–5610.
[49] Vaidya, A.; Jain, S.; Jain, P.; Jain, P.; Tiwari, N.; Jain, R.; Jain, R.; Jain, A. K.; Agrawal, R. K. Synthesis and Biological Activities of Oxadiazole Derivatives: A Review. Mini-Reviews in Medicinal Chemistry **2016**, 16 (10), 825–845.
[50] Wang, J. F.; Jabbour, G. E.; Mash, E. A.; Anderson, J.; Zhang, Y.; Lee, P. A.; Armstrong, N. R.; Peyghambarian, N.; Kippelen, B. Oxadiazole Metal Complex for Organic Light-Emitting Diodes. Advanced Materials **1999**, 11 (15), 1266–1269.
[51] Richardson, C.; Steel, P. J.; Dalessandro, D. M.; Junk, P. C.; Keene, F. R. Mono- and Di-Nuclear Complexes of the Ligands 3,4-Di(2-Pyridyl)-1,2,5-Oxadiazole and 3,4-Di(2-Pyridyl)-1,2,5-Thiadiazole; New Bridges Allowing Unusually Strong Metal–Metal Interactions. Journal of the Chemical Society, Dalton Transactions **2002**, No. 13, 2775–2785.
[52] Janghouri, M.; Mohajerani, E.; Amini, M. M.; Najafi, E.; Hosseini, H. Yellow–Orange Electroluminescence of Novel Tin Complexes. Journal of Electronic Materials **2013**, 42 (10), 2915–2925.

[53] Shen, X.-Q.; Zhong, H.-J.; Zheng, H.; Zhang, H.-Y.; Zhao, G.-H.; Wu, Q.-A.; Mao, H.-Y.; Wang, E.-B.; Zhu, Y. Crystal Structure, Thermal Decomposition Kinetics and Antimicrobial Activities of [Zn(Eatz)2(OAc)2] (Eatz=5-Ethyl-2-Amino-1,3,4-Thiadiazole). Polyhedron **2004**, 23 (11), 1851–1857.
[54] Jin, J.; Zhang, W.; Wang, B.; Mu, G.; Xu, P.; Wang, L.; Huang, H.; Chen, J.; Ma, D. Construction of High Tg Bipolar Host Materials with Balanced Electron–Hole Mobility Based on 1,2,4-Thiadiazole for Phosphorescent Organic Light-Emitting Diodes. Chemistry of Materials **2014**, 26 (7), 2388–2395.
[55] DisplaySearch Report Indicates LCD Monitors Overtake CRT Monitors in Q3'04. https://www.businesswire.com/news/home/20041209005289/en/DisplaySearch-Report-LCD-Monitors-Overtake-CRT-Monitors (accessed Jul 9, 2019).
[56] Smith, T. World LCD TV sales overtake CRT revenues. https://www.theregister.co.uk/2006/03/14/world_tv_sales_q4/ (accessed Jul 9, 2019).
[57] Sherwood, J. Global LCD TV sales overtake CRT. https://www.theregister.co.uk/2008/02/22/displaysearch_crt_lcd_global_q4/ (accessed Jul 9, 2019).
[58] I.D. Parker et al., Society of Information Display International Symposium Digest of Technical Papers **1998**, 29 (15).
[59] Kim, K.-H.; Song, J.-K. Technical Evolution of Liquid Crystal Displays. NPG Asia Materials **2009**, 1 (1), 29–36.
[60] Yoneya, M.; Utsumi, Y.; Umeda, Y. Depolarized Light Scattering from Liquid Crystals as a Factor for Black Level Light Leakage in Liquid-Crystal Displays. Journal of Applied Physics **2005**, 98 (1), 016106.
[61] Physical Properties of Liquid Crystals: Nematics; Dunmur, D., Fukuda, A., Luckhurst, G., Eds.; Institution of Electrical Engineers: London, 2000.
[62] Boher, P.; Bignon, T.; Leroux, T. Angle of View Polarization Characterization of Liquid Crystal Displays and Their Components. Journal of Information Display **2007**, 8 (4), 10–14.
[63] Fujitsu Microelectronics America, Inc. Fundamentals of Liquid Crystal Displays – How They Work and What They Do. https://www.fujitsu.com/downloads/MICRO/fma/pdf/LCD_Backgrounder.pdf (accessed Apr 26, 2020).
[64] Hermann, C. Transparent Displays Functionality explained - Part I. https://www.mmt.io/transparent-lcd-news/transparent-displays-explained-part-1/ (accessed May 27, 2020).
[65] Helfrich, W.; Schneider, W. G. Recombination Radiation in Anthracene Crystals. Physical Review Letters **1965**, 14 (7), 229–231.

[66] Hüttner, J., Kuhn, G., Winter, M. LED Backlighting of LCDs in Mobile Applications. In: Mobile Displays: Technology and Applications; Bhowmik, A. K., Li, Z., Bos, P. J., Eds.; John Wiley & Sons:Chichester, England, **2008**.

[67] Bluesharkslee. OLED 발광원리. https://commons.wikimedia.org/wiki/File:OLED_발광원리.gif (accessed May 26, 2020).

[68] Segal, M.; Baldo, M. A.; Holmes, R. J.; Forrest, S. R.; Soos, Z. G. Excitonic Singlet-Triplet Ratios in Molecular and Polymeric Organic Materials. Physical Review B **2003**, 68 (7).

[69] Tsai, Y., Chang, J., Peng, D., Tseng, V., Lin, A., Chen, L. and Lu, P. Advances in AMOLED Technologies. In: Mobile Displays: Technology and Applications; Bhowmik, A. K., Li, Z., Bos, P. J., Eds.; John Wiley & Sons:Chichester, England, **2008**.

[70] Dresner, J. Double Injection Electroluminescence in Anthracene. RCA Rev. **1969**, 30, 322–344.

[71] Williams, D.; Schadt, M. A Simple Organic Electroluminescent Diode. Proceedings of the IEEE **1970**, 58 (3), 476–476.

[72] Tang, C. W.; VanSlyke, S. A. Organic Electroluminescent Diodes. Applied Physics Letters **1987**, 51 (12), 913–915.

[73] Yang, G.; Su, T.; Shi, S.; Su, Z.; Zhang, H.; Wang, Y. Theoretical Study on Photophysical Properties of Phenolpyridyl Boron Complexes. The Journal of Physical Chemistry A **2007**, 111 (14), 2739–2744.

[74] Seong, T.-Y. Organic Light-Emitting Diodes. http://oemd.korea.ac.kr/3_research_sub_2.php (accessed May 27, 2020).

[75] Mertens, R. Samsung progresses with its inkjet printing OLED technology, to apply it to next-generation monitors and laptops. https://www.oled-info.com/samsung-progresses-its-inkjet-printing-oled-technology-apply-it-next-generation-monitors-and-laptops (accessed Jan 26, 2020).

[76] Im, Y.; Byun, S. Y.; Kim, J. H.; Lee, D. R.; Oh, C. S.; Yook, K. S.; Lee, J. Y. Recent Progress in High-Efficiency Blue-Light-Emitting Materials for Organic Light-Emitting Diodes. Advanced Functional Materials **2017**, 27 (13), 1603007.

[77] Chen, W.-C.; Lee, C.-S.; Tong, Q.-X. Blue-Emitting Organic Electrofluorescence Materials: Progress and Prospective. Journal of Materials Chemistry C **2015**, 3(42), 10957–10963.

[78] Wakamiya, A.; Taniguchi, T.; Yamaguchi, S. Intramolecular B–N Coordination as a Scaffold for Electron-Transporting Materials: Synthesis and Properties of Boryl-Substituted Thienylthiazoles. Angewandte Chemie **2006**, 118 (19), 3242–3245.

[79] Wakamiya, A.; Mori, K.; Yamaguchi, S. 3-Boryl-2,2′-Bithiophene as a Versatile Core Skeleton for Full-Color Highly Emissive Organic Solids. Angewandte Chemie **2007**, 119 (23), 4351–4354.
[80] Wang, S. Luminescence and Electroluminescence of Al(III), B(III), Be(II) and Zn(II) Complexes with Nitrogen Donors. Coordination Chemistry Reviews **2001**, 215 (1), 79–98.
[81] Wu, Q.; Esteghamatian, M.; Hu, N.-X.; Popovic, Z.; Enright, G.; Tao, Y.; D'lorio, M.; Wang, S. Synthesis, Structure, and Electroluminescence of BR2q (R = Et, Ph, 2-Naphthyl and q = 8-Hydroxyquinolato). Chemistry of Materials **2000**, 12 (1), 79–83.
[82] Anderson, S.; Weaver, M. S.; Hudson, A. J. Materials for Organic Electroluminescence: Aluminium vs. Boron. Synthetic Metals **2000**, 111-112, 459–463.
[83] Qin, Y.; Kiburu, I.; Shah, S.; Jäkle, F. Luminescence Tuning of Organoboron Quinolates through Substituent Variation at the 5-Position of the Quinolato Moiety. Organic Letters **2006**, 8 (23), 5227–5230.
[84] Qin, Y.; Jäkle, F. Silylated Initiators for the Efficient Preparation of Borane End-Functionalized Polymers. Macromolecules **2006**, 39, 9041–9048.
[85] Nagata, Y.; Chujo, Y. Main-Chain-TypeN,N′-Chelate Organoboron Aminoquinolate Polymers: Synthesis, Luminescence, and Energy Transfer Behavior. Macromolecules **2008**, 41 (10), 3488–3492.
[86] Ugolotti, J.; Hellstrom, S.; Britovsek, G. J. P.; Jones, T. S.; Hunt, P.; White, A. J. P. Synthesis and Characterisation of Luminescent Fluorinated Organoboron Compounds. Dalton Transactions **2007**, No. 14, 1425.
[87] Loudet, A.; Burgess, K. BODIPY Dyes and Their Derivatives: Syntheses and Spectroscopic Properties. Chemical Reviews **2007**, 107 (11), 4891–4932.
[88] Zhang, H.; Huo, C.; Ye, K.; Zhang, P.; Tian, W.; Wang, Y. Synthesis, Structures, and Luminescent Properties of Phenol−Pyridyl Boron Complexes. Inorganic Chemistry **2006**, 45 (7), 2788–2794.
[89] Yang, G.; Su, T.; Shi, S.; Su, Z.; Zhang, H.; Wang, Y. Theoretical Study on Photophysical Properties of Phenolpyridyl Boron Complexes. The Journal of Physical Chemistry A **2007**, 111 (14), 2739–2744.
[90] Organic Light-Emitting Materials and Devices, 2nd Rev. ed.; Li, Z. R., Meng, H. R., Eds.; CRC Press, Taylor & Francis Group: Boca Raton, FL, 2015.
[91] Wakamiya, A.; Mori, K.; Yamaguchi, S. 3-Boryl-2,2′-Bithiophene as a Versatile Core Skeleton for Full-Color Highly Emissive Organic Solids. Angewandte Chemie International Edition **2007**, 46 (23), 4273–4276.
[92] Kappaun, S.; Rentenberger, S.; Pogantsch, A.; Zojer, E.; Mereiter, K.; Trimmel, G.; Saf, R.; Möller, K. C.; Stelzer, F.; Slugovc, C. Organoboron Quinolinolates with Extended Conjugated Chromophores: Synthesis, Structure,

and Electronic and Electroluminescent Properties. Chemistry of Materials **2006**, 18 (15), 3539–3547.
[93] Jia, W.-L.; Song, D.; Wang, S. Blue Luminescent Three-Coordinate Organoboron Compounds with a 2,2‘-Dipyridylamino Functional Group. The Journal of Organic Chemistry **2003**, 68 (3), 701–705.
[94] Cui, Y.; Wang, S. Diboron and Triboron Compounds Based on Linear and Star-Shaped Conjugated Ligands with 8-Hydroxyquinolate Functionality: Impact of Intermolecular Interaction and Boron Coordination on Luminescence. The Journal of Organic Chemistry **2006**, 71 (17), 6485–6496.
[95] Kiprof, P.; Carlson, J. C.; Anderson, D. R.; Nemykin, V. N. Systematic Color Tuning of a Family of Luminescent Azole-Based Organoboron Compounds Suitable for OLED Applications. *Dalton Transactions* **2013**, *42* (42), 15120.
[96] Hines, J. W. Strategic Synthetic Color Tuning of Oxadiazole Based Luminescent Organoboron Compounds. Masters, University of Minnesota, Duluth, MN, 2016.
[97] Frath, D.; Massue, J.; Ulrich, G.; Ziessel, R. Luminescent Materials: Locking π-Conjugated and Heterocyclic Ligands with Boron(III). *Angewandte Chemie International Edition* **2014**, *53* (9), 2290–2310.
[98] Lakowicz, J. R. *Principles of Fluorescence Spectroscopy*, 3rd ed.; Springer: New York, 2006.
[99] Lebrini,, M.; Bentiss, F.; Lagrenee, M. Rapid Synthesis of 2,5-Disubtituted 1,3,4-Thiadiazoles under Microwave Irradiation. *Journal of Heterocyclic Chemistry* **2005**, *42* (5), 991–994.

Appendix

All supporting spectra are provided herein. Refer to table to contents for pagination.

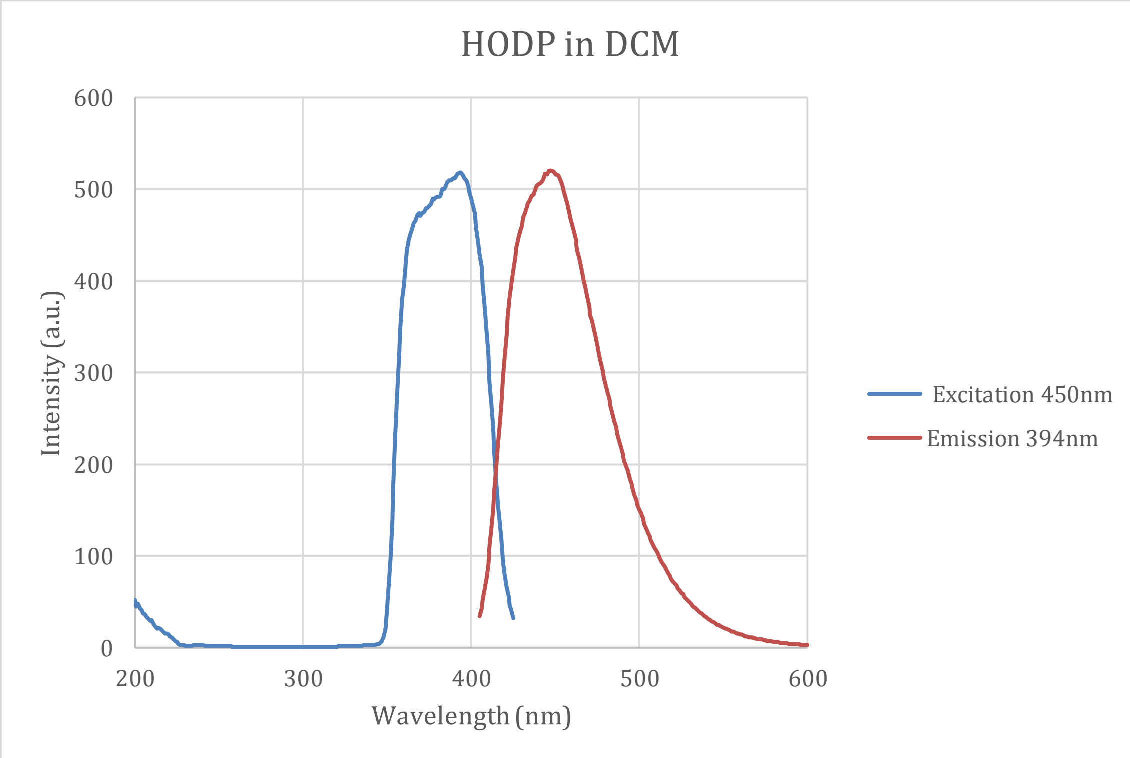

Figure 13 Excitation and emission data for HODP in DCM

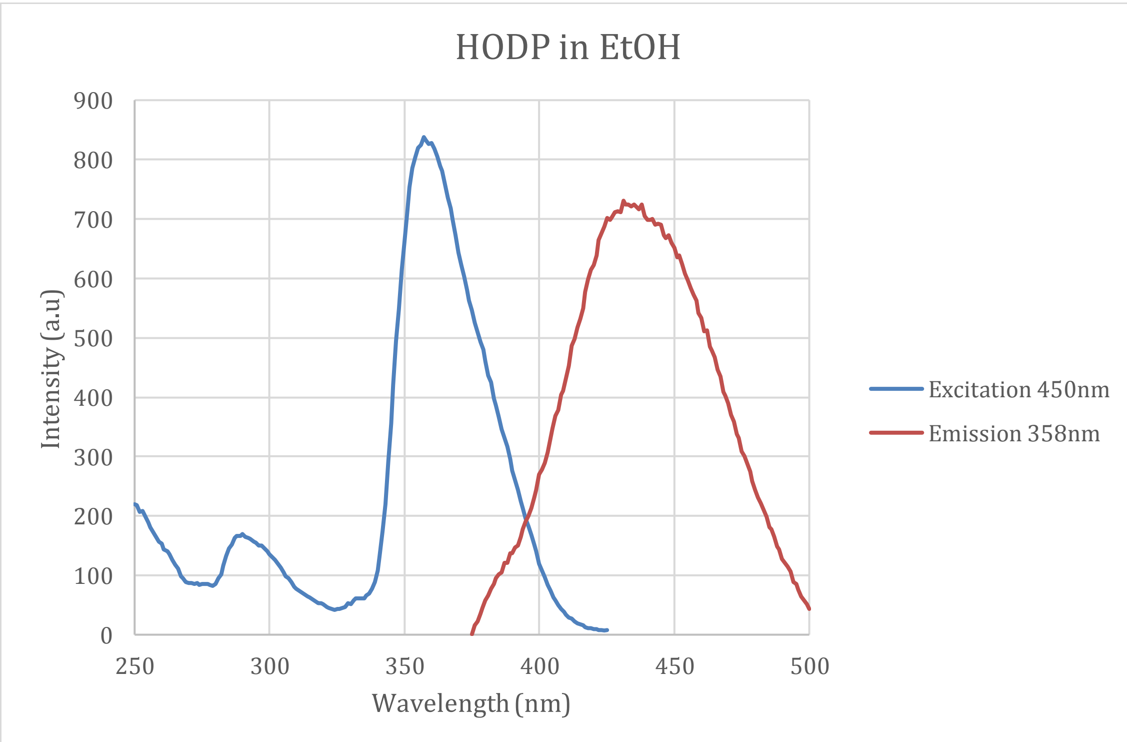

Figure 14 Excitation and emission data for HODP in ethanol

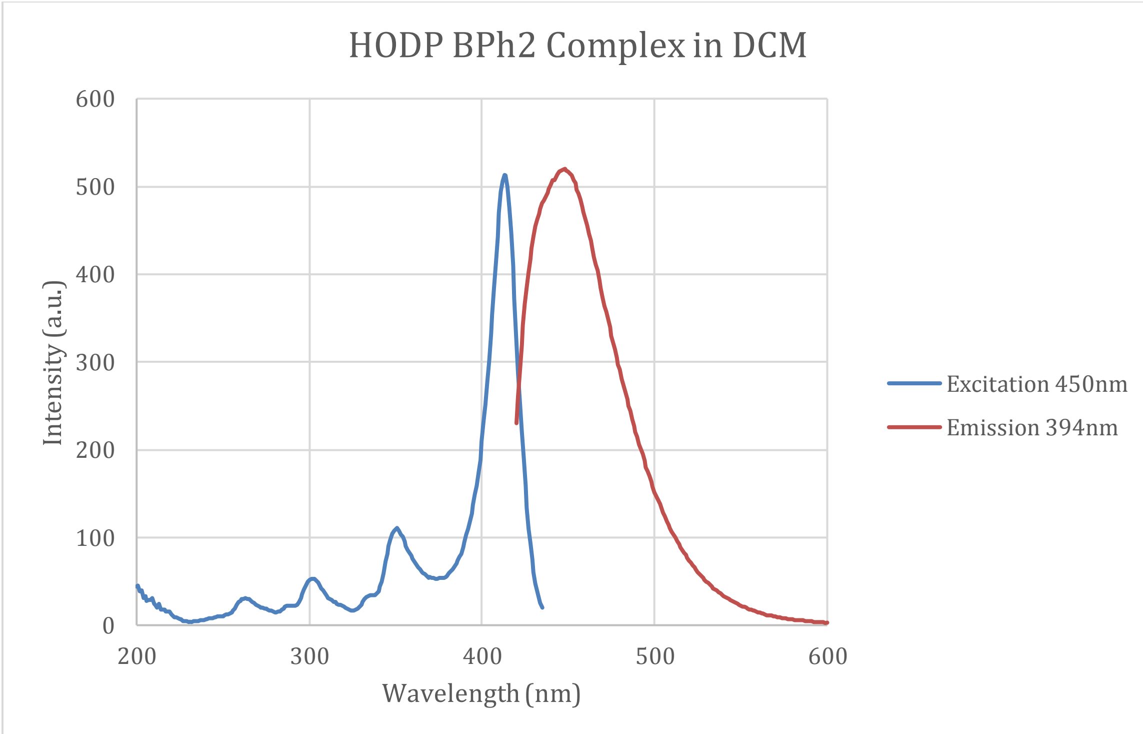

Figure 15 Excitation and emission data for BPh_2(ODP) in DCM

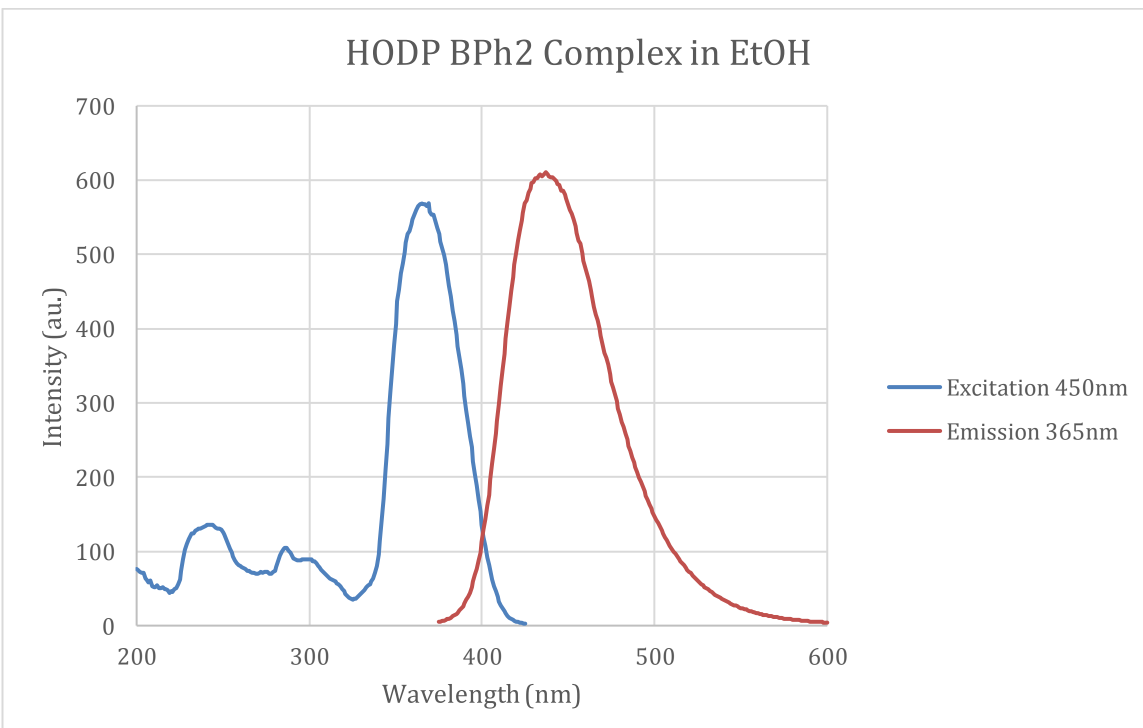

Figure 16 Excitation and emission data for BPh_2(ODP) in ethanol

NMR Spectroscopy

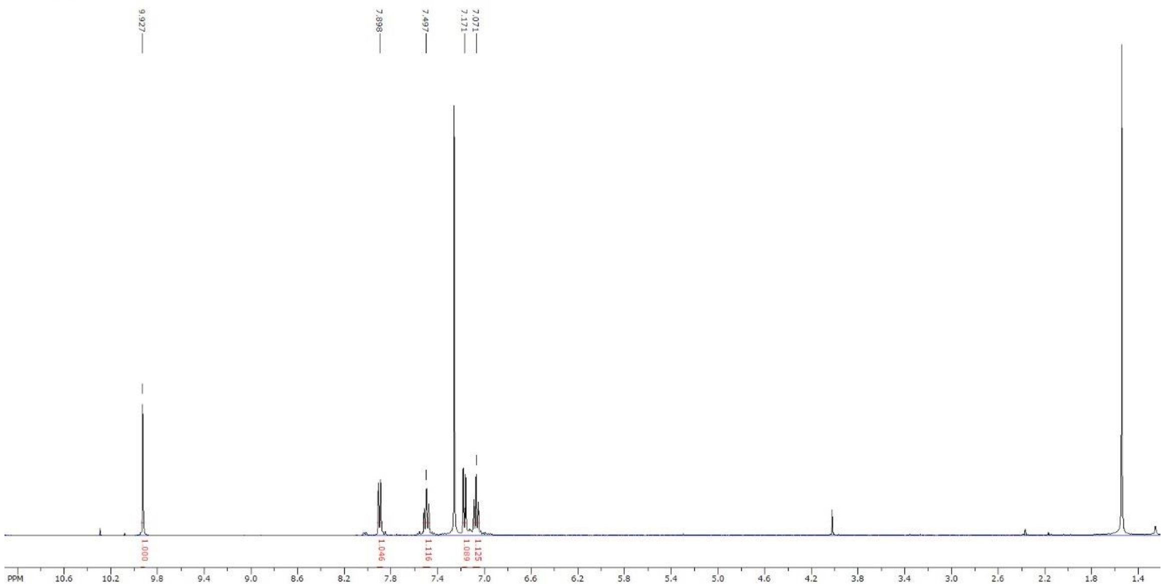

Figure 17 ^{1}H NMR 2,2'-(1,3,4-oxadiazole-2,5-diyl)diphenol (400 MHz, $CDCl_3$) δ 9.927, 7.898, 7.497, 7.171, 7.071

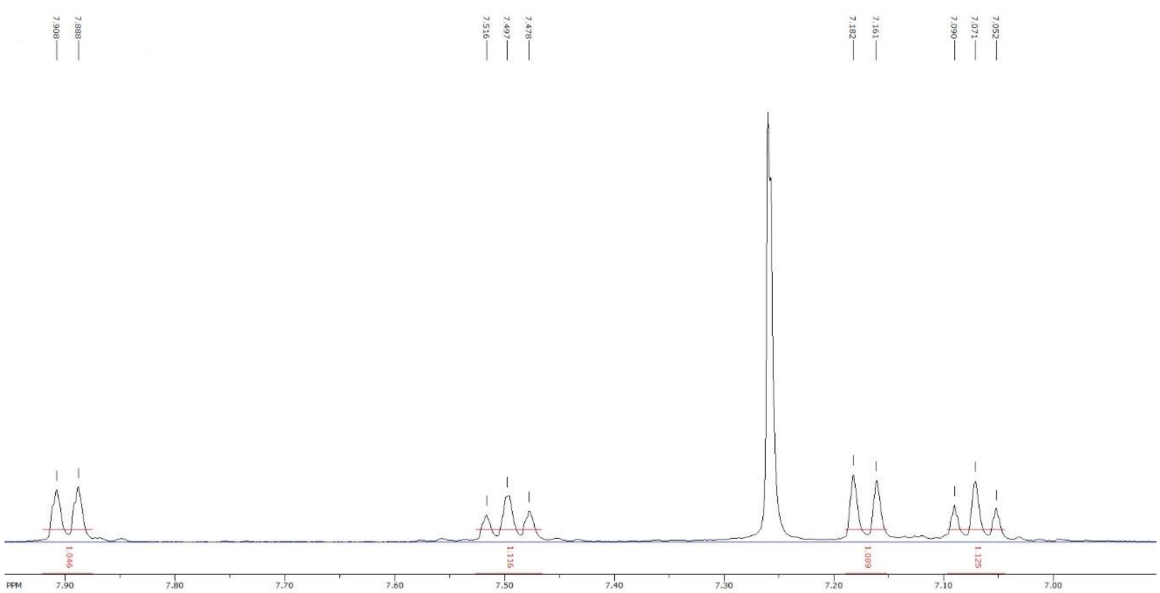

Figure 18 ^{1}H NMR 2,2'-(1,3,4-oxadiazole-2,5-diyl)diphenol (400 MHz, $CDCl_3$) δ 7.908, 7.888, 7.516, 7.497, 7.478, 7.182, 7.161, 7.090, 7.071, 7.052

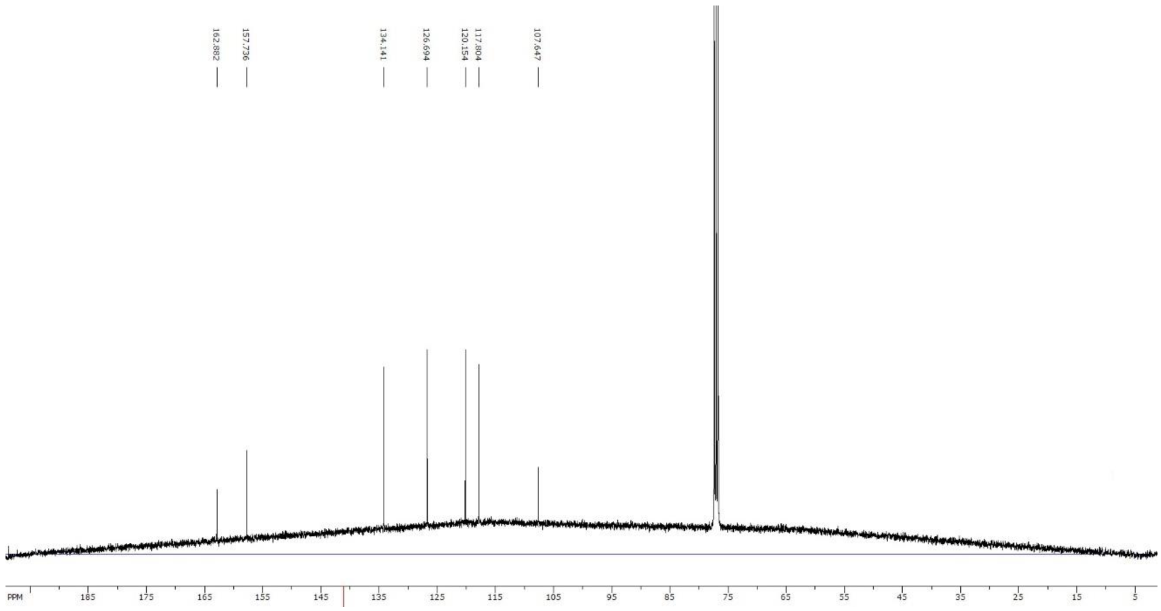

Figure 19 ^{13}C NMR 2,2'-(1,3,4-oxadiazole-2,5-diyl)diphenol (400 MHz $CDCl_3$) δ 162.88, 157.74, 134.14, 126.69, 120.15, 117.80, 107.65

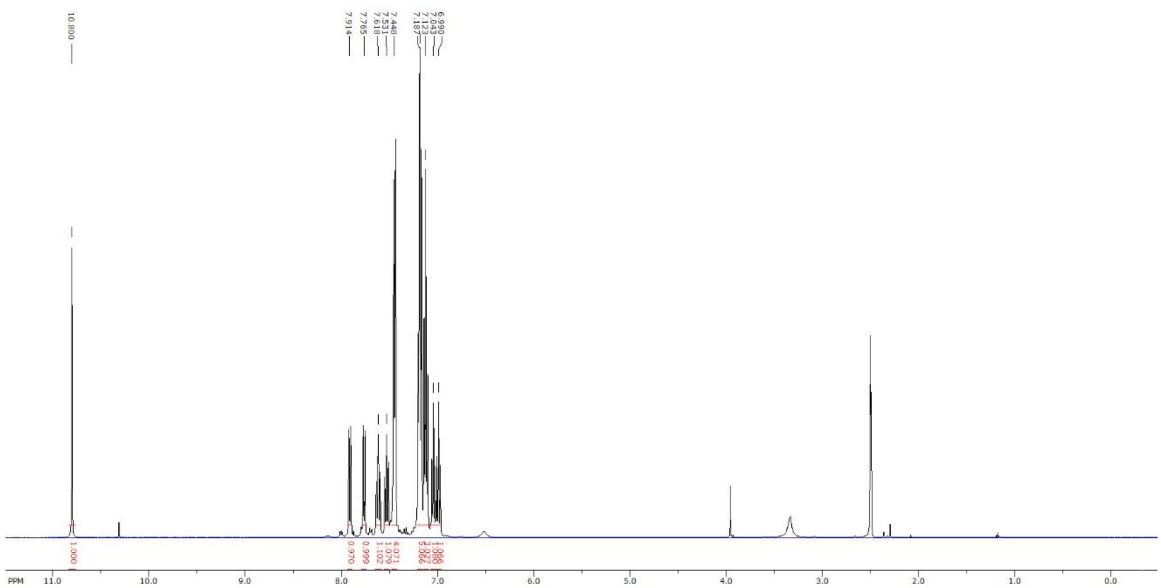

Figure 20 ^{1}H NMR 2-(4-(2-((diphenylboryl)oxy)phenyl)cyclopenta-1,3-dien-1-yl)phenol (400 MHz, DMSO) δ 10.800, 7.914, 7.765, 7.618, 7.531, 7.448, 7.187, 7.123, 7.043, 6.990

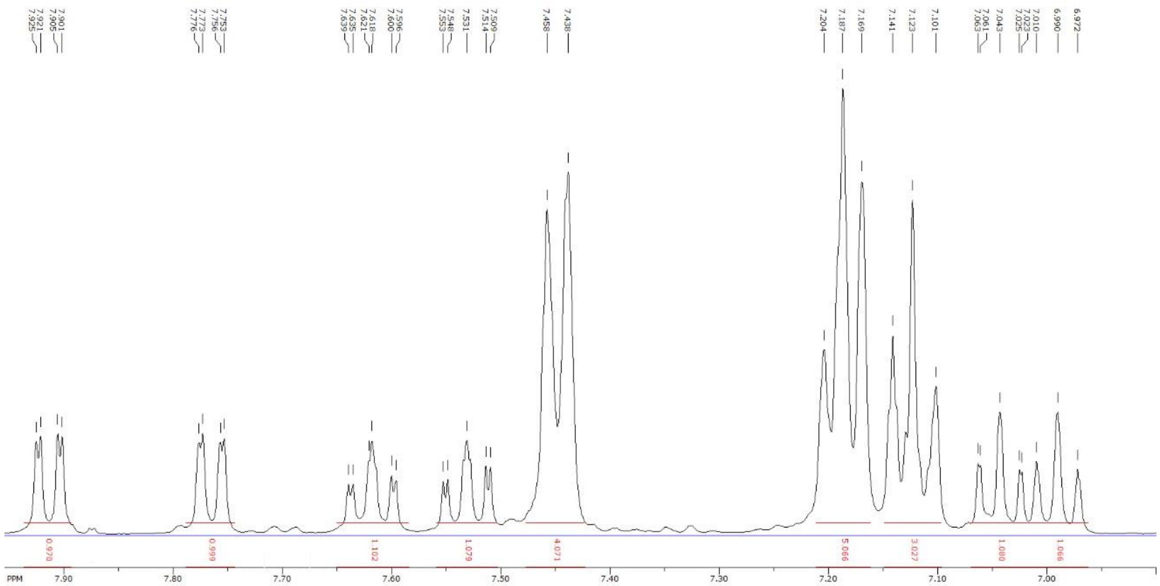

Figure 21 ^{1}H NMR 2-(4-(2-((diphenylboryl)oxy)phenyl)cyclopenta-1,3-dien-1-yl)phenol (400 MHz, DMSO) δ 7.925, 7.921, 7.905, 7.901, 7.776, 7.773, 7.756, 7.753, 7.639, 7.635, 7.621, 7.618, 7.600, 7.596, 7.553, 7.548, 7.531, 7.514, 7.509, 7.458, 7.438

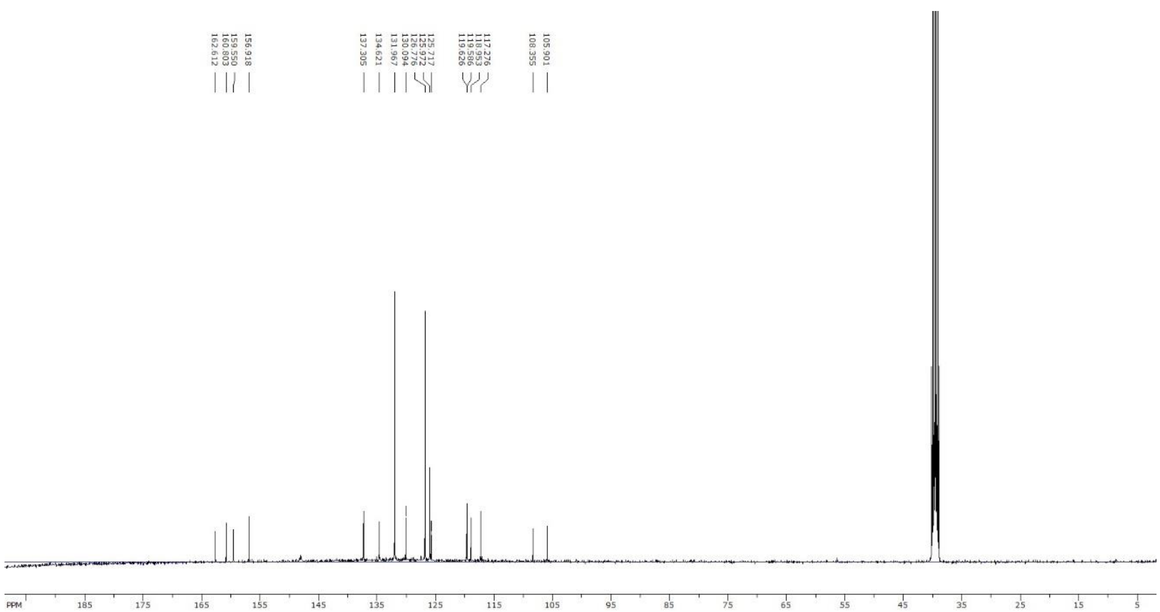

Figure 22 ^{13}C NMR 2-(4-(2-((diphenylboryl)oxy)phenyl)cyclopenta-1,3-dien-1-yl)phenol (400 MHz, DMSO) δ 162.61, 160.80, 159.55, 156.92, 137.31, 134.62, 131.97, 130.09, 126.78, 125.97, 125.72, 119.63, 119.59, 118.95, 117.28, 108.36, 105.90

LCMS Spectroscopy

Generic Display Report

Analysis Info

Analysis Name	D:\Data\KiprofLab\SamData\R5 HPOP S2 ESI neg_RE1_01_3318.d	Acquisition Date	2/14/2020 3:05:46 PM
Method	ESI_Neg_LowTune.m	Operator	BDAL@DE
Sample Name	R5 HPOP S2 ESI neg	Instrument	micrOTOF-Q III
Comment			

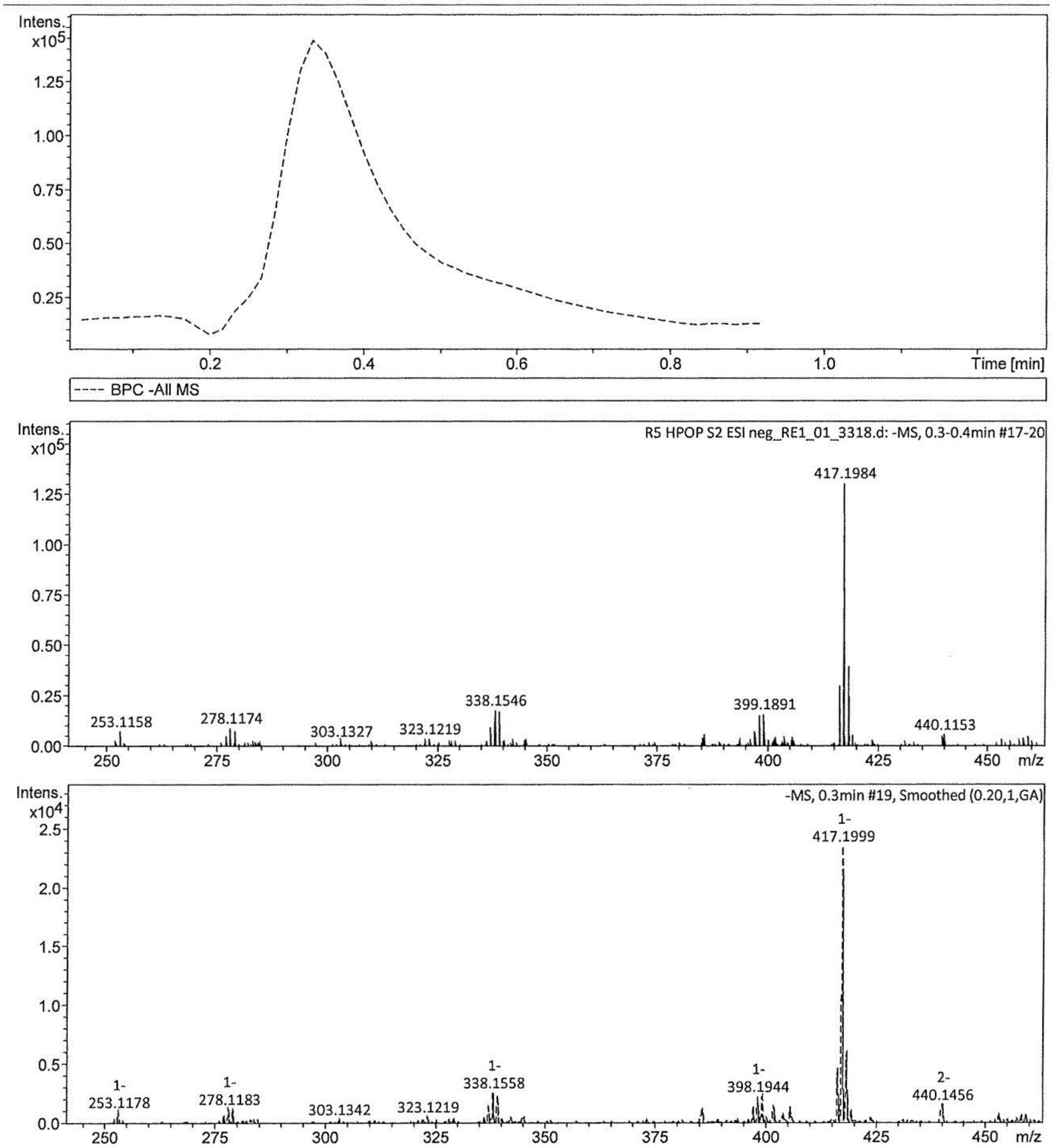

Bruker Compass DataAnalysis 4.2 printed: 3/18/2020 4:20:54 PM by: BDAL@DE Page 1 of 1

Figure 23 LCMS of BPh_2(ODP)

GCMS Spectroscopy

Operator : SS
Acquired : 30 May 2019 11:00 using AcqMethod 12M-METHOD-1.M
Instrument : GCMS301
Sample Name: R2 HPOP S5 E1 WHITE
Misc Info : WHITE FLUFF IN DCM
V Number: 1

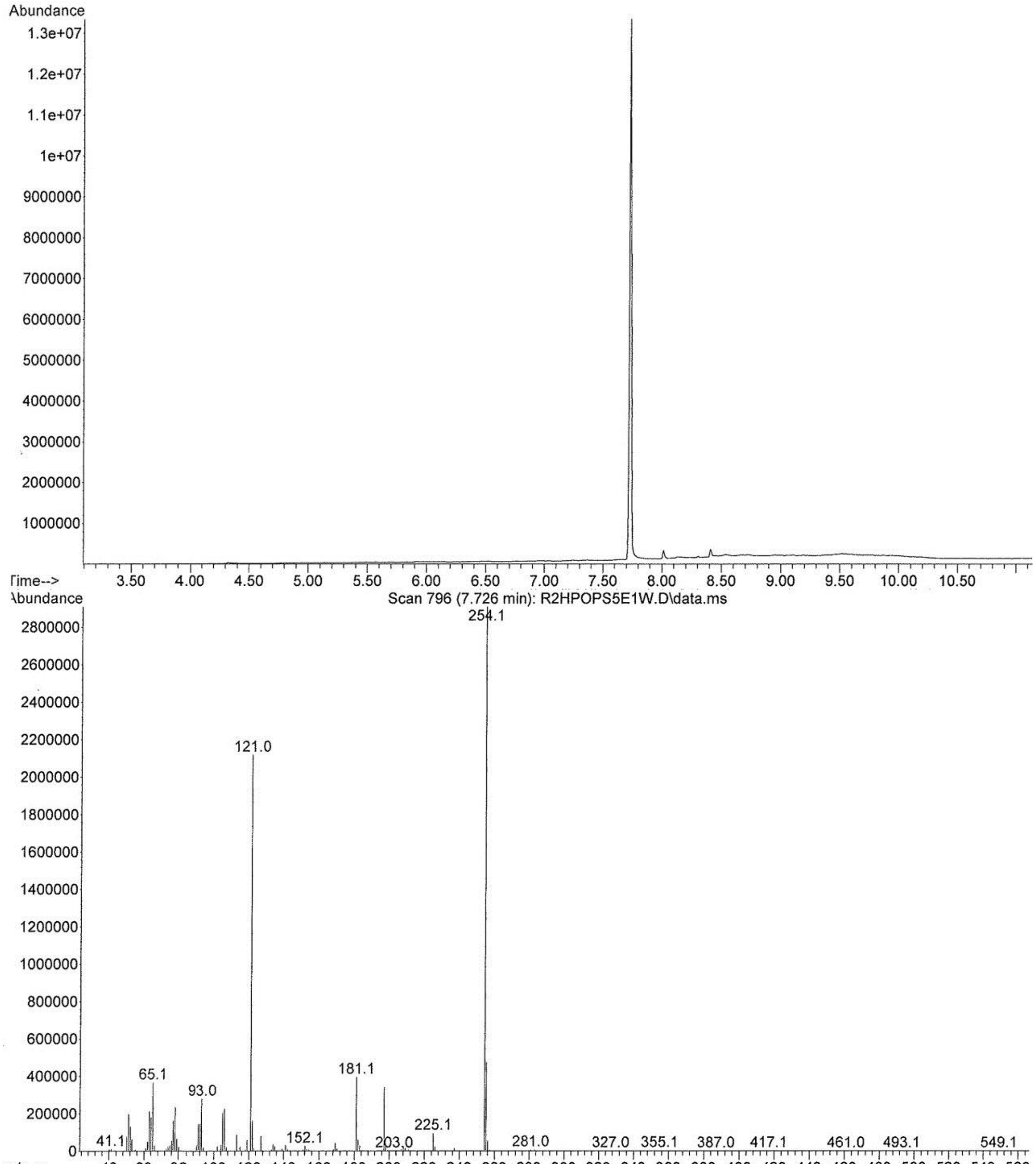

Figure 24 GCMS of HODP